III. THE STRUCTURE

III.A. INTRODUCTION TO IMAGE PROCESSING OF BIOLOGICAL SPECIMENS

The terms **image analysis** and **image processing** are often incorrectly assumed to be synonymous, but they refer to different aspects of the treatment of image data. **Image analysis** involves the quantification and classification of images and objects of interest within images. **Image processing** refers to any technique that alters and displays, in more tangible form, the information contained in images. An image might be analyzed either before or after it has been processed. Most of this class is devoted to learning about the methods by which electron micrograph images can be processed to obtain clearer images of biological macromolecules photographed at high magnifications.

Reversal of image contrast when a positive print is made from a photographic negative represents, perhaps, the simplest and most practiced form of image processing. More sophisticated techniques were developed in the 1960s (led by Robert Nathan at the Jet Propulsion Laboratory) to enhance images of the moon and other celestial objects. Markham, *et al.* (1963) and Klug and Berger (1964) were the first to develop processing techniques to study the structures of biological specimens imaged by electron microscopy. They succeeded in separating structural details relating to the regular features of periodic specimens (**SIGNAL**), from non-regular details (**NOISE**). A primary goal of biological, electron micrograph image processing is to extract accurate structural information from specimen images that are obscured with noise (§ III.B).

Image processing extends the electron microscopist's ability to study imaged biological structure because details that may be invisible to the naked eye can be clearly revealed. An obvious benefit of the clearer images and structural information is an enhanced understanding of biological structure-function relationships. Correlation with X-ray diffraction, biochemical, genetic, immunological, and model building studies makes image processing a powerful tool for investigating the basis of molecular events in living systems.

III.A.1. Image Processing Techniques: Real and Reciprocal Space Methods

Since 1963 several techniques have been developed and are now routinely used in biological structure studies. Optical and computer diffraction and filtering, three-dimensional (3D) reconstruction, rotational and translational optical superposition, real space iteration and back-projection, correlation and convolution averaging, and holographic methods are among many that have been or are available. Not surprisingly, certain techniques are better suited than others for studying some specimens. Image processing techniques are classified as either **real-space** (direct) or **reciprocal-space** (Fourier) depending on whether the micrograph itself is processed or an intermediate step involving the Fourier transformation of the micrograph is required for processing. The main emphasis in this course concerns the Fourier analysis and processing of periodic specimens because Fourier techniques are well established and have been used extensively to study a wide variety of periodic biological systems. As time permits, other, popular techniques will be introduced.

III.A.2. Fourier Image Processing

Fourier image processing, based on the well established principles of X-ray diffraction and X-ray crystallography, was primarily developed in the 1960's and 1970's by A. Klug and colleagues at the Medical Research Council Laboratory in Cambridge, England, and has been the technique of choice in a majority of structural studies of biological macromolecular assemblies. Fourier techniques are most effective for the study of crystalline or paracrystalline specimens. However, in principle, these techniques can be applied to the study of any non-crystalline specimen. Fortunately, a wide range of biological specimens naturally occur or can be isolated *in vitro* as regular arrays and are amenable to this type analysis. Viruses, muscle proteins, membranes, ribosomes, flagella, microtubules, enzymes, pili, chromatin, etc. have all been successfully examined by Fourier-based image processing techniques.

Fourier processing may be performed **optically** on an optical bench or **digitally** on a computer. Both techniques have distinct advantages and disadvantages that are discussed later (§ III.D.3.b).

It should be emphasized, however, that there are other quite powerful and quantitative techniques such as correlation methods that offer distinct advantages over Fourier techniques for examining certain kinds of specimens (*e.g.* disordered or non-periodic specimens). If time permits, some of these techniques will be discussed.

III.A.3. Periodic/Non-Periodic Specimens

Except where noted, we will concentrate on studies of **ordered specimens** (*i.e.* containing regular arrangement of "subunits"), and **specimens prepared by conventional negative staining or cryo-microscopy techniques** imaged under normal or minimal exposure conditions of bright field transmission electron microscopy (100-400 keV at 10,000-100,000X). The fundamentals of Fourier (diffraction) theory and related topics are discussed in § III.C.4 to help facilitate more effective application of Fourier techniques and to identify the capabilities and limitations of the techniques. Literature references provide the rigorous mathematical treatments omitted here in favor of more illustrative descriptions. Inherent assumptions and the effects of sample preparation and imaging are discussed (§ III.F) to emphasize ways to improve the quality and significance of results obtained by image processing. Technical details of optical diffraction (§ III.D.1) and filtering (§ III.D.2) are compared with other analysis methods (§ III.D.3.b and III.G). § III.H discusses the display and interpretation of final results.

III.A.4. Applications and Advantages of Image Analysis/Processing

The following list identifies many of the common uses of image analysis/processing.

a. Objective means to reveal, assess, and measure periodic structural detail.

Lattice dimensions (unit cell size and shape) are more accurately measured than by direct means. Dimensions aid in estimating molecular weights and identifying chemical species.

Detection of rotational and translational symmetry elements.

Detection of specimen preservation (distortion, resolution, staining artifacts). This provides a good criteria for selecting suitable images for further analysis. Some types of specimen distortions (*e.g.* crystal lattice distortions) can be reduced or removed with specific analysis techniques.

Determine average positions, size, and shape of subunits.

Identify and separate signal and noise components in images.

Separate Moiré images from multi-layered specimens.

b. Use image averaging to improve contrast, reduce noise, and improve resolution over what could be obtained in a single image. Averaging allows particular specimen features to be enhanced.

c. Recover (reconstruct) 3D information from 2D images.

d. Determine and adjust the imaging conditions and assess the quality and conditions of microscopy (astigmatism, focusing, specimen, and focal drift, and beam coherence).

e. Determine handedness of structures.

f. Measure specimen thickness.

g. Determine or verify chemical stoichiometries.

h. Detect conformational changes in macromolecules.

i. Study macromolecular assembly and the molecular events leading to movement.

j. Perform image restoration operations - (deblurring, contrast stretching, histogram equalization, low and high-pass frequency filtering, etc.).

k. Teaching aid for understanding diffraction theory and methods.

III.A.5. References Cited in §III.A.

Klug, A. and J. E. Berger (1964) An optical method for the analysis of periodicities in electron micrographs, and some observations on the mechanism of negative staining. *J. Mol. Biol.* **10:565-569.**

Markham, R., S. Frey, and G. J. Hills (1963) Methods for the enhancement of image detail and accentuation of structure in electron microscopy. *Virology* **20:88-102.**

III.B. SOURCES OF NOISE IN TEM IMAGES OF BIOLOGICAL SPECIMENS

Noise appears in all micrographs to varying extents and can arise from a variety of sources. **Image processing** methods **identify and separate signal and noise components** in the image. Four major sources of noise include the specimen and specimen support film, the microscope, and photography. Each of these is briefly discussed below.

III.B.1. Specimen

The specimen observed in the microscope environment may not bear a close resemblance to the "native" state for any of several reasons:

a. **Impurities in the sample** such as the presence of minor contaminants (*e.g.* extra protein) in the specimen sample used for microscopy.

b. **Inherent disorder or irregularities** at the atomic, molecular, or macromolecular levels.

c. **Induced disorder** caused by the preparation and imaging procedures, for example, from radiation damage, dehydration effects, or stain-induced effects (*i.e.* unfavorable interaction with stains and variability and granularity of stains).

d. **Contamination** buildup from beam-induced fixation of volatile molecules in the microscope column to the specimen or **etching** due to interaction of the specimen with ions or free radicals produced by the interaction of the electron beam with water molecules in the microscope column (see § II.B.4.b).

III.B.2. Specimen Support Film

Variability in the specimen support film produces the so-called "phase-granularity" (fine, background substructure) superimposed on the specimen image. Variability can arise from unevenness in the film since it is unlikely to be "perfectly" flat and uniformly thick. It is also quite possible that the specimen under observation may be tilted by as many as a few degrees with respect to the electron beam because the underlying support film may itself be tilted. Recall that image contrast, and hence visibility of specimen features, is reduced as the support film thickness increases relative to the specimen.

III.B.3. Microscope

As was outlined in **§ I** (**THE MICROSCOPE**), several factors related to microscopy affect the recorded image of the specimen indicating there is a non-simple relationship between the micrograph and specimen. Some of the more significant factors include:

Spherical and **chromatic aberration** in the objective lens

Defocus level of the objective lens (leading to phase contrast effects)

Astigmatism in the objective lens

Thermal drift/Mechanical vibrations

Electrostatic charging (usually in specimens thicker than 50 nm)

Electron statistics (random arrival of electrons)

Random scattering of electrons from the internal parts of the microscope

III.B.4. Analog or Digital Photography

Granularity of the **photographic emulsion** limits resolution of the electron image and results in a non-linear contrast transfer function

Non-linear exposure and **development conditions.**

Readout and thermal noise in CCD and DDD detedtors and the pulse-width

distribution of CCD detectors.

Image processing may be successfully applied whether or not specific sources of noise are identified or quantitated. Nevertheless, processing is more likely to produce meaningful results and is easier to apply if attempts are made to reduce as many sources of noise as possible **during** specimen preparation and microscopy as indicated in Sections I (**THE MICROSCOPE**) and II (**THE SPECIMEN**).

III.C. CRYSTALS, SYMMETRY, AND DIFFRACTION

Biomacromolecules quite often occur naturally or *in vitro* as organized structures composed of subunits arranged in a symmetrical way. Such structures are readily studied by diffraction methods. The fundamental concepts concerning crystalline matter, symmetry relationships, and diffraction theory form a basic framework for understanding the principles and practice of image processing and interpretation of structural results. The main concepts, summarized here, are presented in more detailed, introductory form in excellent texts such as Eisenberg and Crothers (1979), Glusker and Trueblood (1972), Holmes and Blow (1965), Sherwood (1976), and Wilson (1966). For additional references, see the Reading List posted on the course Web site.

III.C.1. Definitions of Terms (compiled from Glusker & Trueblood, and Eisenberg & Crothers)

Asymmetric Unit: Part of the symmetric object from which the whole is built up by repeats. Thus, it is the smallest unit from which the object can be generated by the symmetry operations of its point group. Fig. III.3.

Bravais lattice: One of the 14 possible arrays of points repeated periodically in 3D space in such a way that the arrangement of points about any one of the points in the array is identical in every respect to that about any other point in the array. Fig. III.2.

Center of Symmetry (or Center of Inversion): A point through which an inversion operation (*i*) is performed, converting an object into its mirror image. Fig. III.10.

Crystal: A solid having a regularly repeating internal arrangement of its atoms. Figs. III.5-7.

Crystal lattice: Crystals are composed of groups of atoms repeated at regular intervals in three dimensions with the same orientation. For certain purposes it is sufficient to regard each such group of atoms as replaced by a representative point; the collection of points so formed is the space lattice or lattice of the crystal. Each crystal lattice is a Bravais lattice. Figs. III.1, 2, 4, and 7.

Crystal Structure: The mutual arrangement of atoms, molecules or ions that are packed together in a lattice to form a crystal. Figs. III.5-7.

Crystal System: The seven crystal systems, best classified in terms of their symmetry, correspond to the seven fundamental shapes for unit cells consistent with the 14 Bravais lattices. Fig. III.2 and Table III.2.

Glide Plane: A symmetry element for which the symmetry operation is reflection across the plane combined with translation in a direction parallel to the plane. Figs. III.28-29.

Improper Rotation: The combination of a rotation with either an inversion (*i*), or a reflection (*m*) in the plane perpendicular to the rotation axis. Figs. III.12 and III.13b.

Inversion (*i*): A symmetry operation in which each point of an object is converted to an equivalent point by projecting through a common center (called **center of inversion** or **center of symmetry**) and extending an equal distance beyond this center. If the center of symmetry is at the origin of the coordinates, every point *x,y,z* becomes *-x,-y,-z*. It converts an object or a structure into one of opposite "handedness", related to the first as is any object and its mirror image. Figs. III.10 and III.12.

Lattice: Rule for translation. Fig. III.1 and Tables III.1 and III.2.

Mirror Plane (*m*): A symmetry element for which the corresponding symmetry operation ("reflection") resembles reflection in a mirror coincident with the plane. It converts an object or a structure into one of opposite "handedness", related to the first as is any object and its mirror image. Figs. III.10-11.

Motif: Object that is translated. Figs. III.3, 4, and 7.

Plane Group: Symmetry of a two-dimensional structure. There are 17 plane group symmetries possible (only five for biological structures). Figs. III.6 and 23-27.

Point Group: The collection of symmetry operations that describe the symmetry of an object about a point.

Figs. III.8-17.

Reciprocal Lattice: The lattice with axes $\boldsymbol{a^*,b^*,c^*}$ related to the crystal lattice or direct lattice (with axes ***a,b,c***) in such a way that $\boldsymbol{a^*}$ is perpendicular to ***b*** and ***c***; $\boldsymbol{b^*}$ is perpendicular to ***a*** and ***c***; and $\boldsymbol{c^*}$ is perpendicular to ***a*** and ***b***. Rows of points in the direct lattice are normal to nets of the reciprocal lattice, and vice versa. For a given crystal, the direct lattice and reciprocal lattice have the same symmetry. The repeat distance between points in a particular row of the reciprocal lattice is inversely proportional to the interplanar spacing between the nets of the crystal lattice that are normal to this row of points.

Reflection (*m*): A symmetry operation that resembles reflection in a mirror coincident with the plane. It converts an object or a structure into one of opposite "handedness", related to the first as is any object and its mirror image. Figs. III.10 (left) and 11.

Rotation Axis: An axis of symmetry for an object, such as a crystal. When the object is rotated by (360/*n*)° about an *n*-fold rotation axis, the new orientation is indistinguishable from the original one. Figs. III.9 and 12.

Rotary-Inversion Axis: An axis for which the corresponding symmetry operation is a rotation by (360/*n*)° combined with inversion through a center of symmetry lying on the axis. Figs. III.12-13.

Screw Axis: An axis (designated n_m) for which the corresponding symmetry operation is a rotation about the axis by (360/*n*)° followed by a translation parallel to the axis by *m/n* of the unit cell length in that direction. Figs. III.19-21.

Space group: A group or array of operations consistent with an infinitely extended regularly repeating pattern. It is the symmetry of a 3D structure. There are 230 space group symmetries possible (only 65 for biological structures).

Symmetry: An object is symmetric if some spatial manipulation of it results in an indistinguishable object. A symmetric object can be superimposed on itself by some operation.

Symmetry Element: Geometrical entity (such as a line, a point or a plane) about which a symmetry operation is carried out.

Symmetry Operation: The operation that leads to superimposition of an object on itself (*i.e.* results in moving the object to a position in which its appearance is indistinguishable from its initial appearance). Symmetry operations include rotation, inversion, reflection, and translation.

Translation: A motion in which all points of an object move in the same direction, that is, along the same or parallel lines. Fig. III.18.

Unit Cell: The fundamental portion of a crystal structure that is repeated infinitely by translation in three dimensions. It is characterized by three vectors ***a,b,c,*** not in one plane, which form the edges of a parallelepiped. Figs. III.1, 2, and 7.

III.C.2. Crystals

A **crystal** is a regular arrangement of atoms, ions, or molecules, and is conceptually built up by the continuing translational repetition of some structural pattern. This pattern, or **unit cell**, may contain one or more molecules or a complex assembly of molecules. In three dimensions (3D), the unit cell is defined by three edge lengths (*a,b,c*) and three interaxial angles (α,ß,γ). The different **3D crystal systems** (triclinic, monoclinic, orthorhombic, tetragonal, trigonal, hexagonal and cubic) arise from the seven fundamental unit cell shapes. The simplest, triclinic, is a parallelepiped, with no restrictions on cell lengths or angles. A cubic cell has equal (*a=b=c*) and orthogonal (α=ß=γ=90°) edges.

III.C.3. Lattices

A **lattice** is a **mathematical formalism** that defines an infinite array of imaginary points: each point in the lattice is identical to every other point. That is, the view from each point is identical with the view in the same direction from any other point. This condition is not obeyed at the boundary of a finite, but otherwise perfect crystal. The crystal **structure** and the crystal **lattice** are **NOT equivalent:** the structure is an array of **objects** whereas the lattice is an array of **imaginary, infinitely small points.** A 2D lattice is defined by two translations, *a,b,* and two axes at an angle α to each other. A 3D lattice is defined by three translations, *a,b,c,* and three axes at angles α,ß,γ to each other.

Crystal lattices (2D or 3D) may be **primitive,** with one lattice point per unit cell, or **centered,** containing two or four points per cell. The **four 2D lattice systems** (Table III.1) are subdivided into a total of **five 2D lattices** (Fig. III.1). There are **seven 3D crystal systems** corresponding to the seven basic space-filling shapes that unit cells can adopt. These are subdivided into a total of fourteen, so-called **Bravais lattices** (Table III.2 and Fig. III.2). For example, the cubic crystal system includes three Bravais lattices: primitive (*P*), body centered (*I*), and face centered (*F*).

Lattice system	Lattice type	Conventional representation	Representative points
Oblique	*P*	$a \neq b$ $\varphi > 90^\circ$	(0, 0)
Square	*P*	$a = b$ $\varphi = 90^\circ$	(0, 0)
Hexagonal	*P*	$a = b$ $\varphi = 120^\circ$	(0, 0)
Rectangular	*P*	$a \neq b$ $\varphi = 90^\circ$	(0, 0)
	I	$a \neq b$ $\varphi = 90^\circ$	(0, 0), $(\frac{1}{2}, \frac{1}{2})$

Table III.1. Plane lattices. (From Sherwood, 1976, p.70).

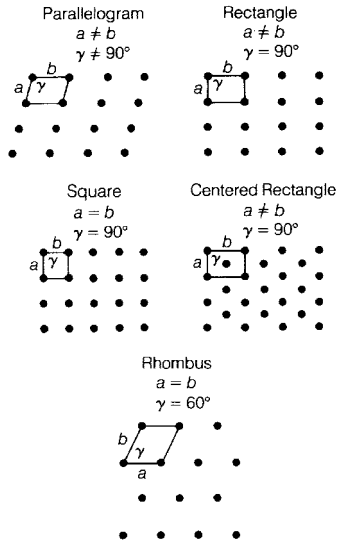

Fig. III.1. The five two-dimensional lattices. (From Eisenberg and Crothers, 1979, p. 786)

Crystal system	Lattice type	Conventional representation	Representative points
Triclinic	*P*	$a \neq b \neq c$ $\alpha \neq \beta \neq \gamma$	(0, 0, 0)
Monoclinic	*P*	$a \neq b \neq c$ $\alpha = \gamma = 90^\circ \neq \beta$	(0, 0, 0)
	I		(0, 0, 0), $(\frac{1}{2}, \frac{1}{2}, \frac{1}{2})$
Orthorhombic	*P*	$a \neq b \neq c$ $\alpha = \beta = \gamma = 90^\circ$	(0, 0, 0)
	C		(0, 0, 0), $(\frac{1}{2}, \frac{1}{2}, 0)$
	I		(0, 0, 0), $(\frac{1}{2}, \frac{1}{2}, \frac{1}{2})$
	F		(0, 0, 0), $(\frac{1}{2}, \frac{1}{2}, 0)$ $(\frac{1}{2}, 0, \frac{1}{2})$, $(0, \frac{1}{2}, \frac{1}{2})$
Tetragonal	*P*	$a = b \neq c$ $\alpha = \beta = \gamma = 90^\circ$	(0, 0, 0)
	I		(0, 0, 0), $(\frac{1}{2}, \frac{1}{2}, \frac{1}{2})$
Cubic	*P*	$a = b = c$ $\alpha = \beta = \gamma = 90^\circ$	(0, 0, 0)
	F		(0, 0, 0), $(\frac{1}{2}, \frac{1}{2}, 0)$ $(\frac{1}{2}, 0, \frac{1}{2})$, $(0, \frac{1}{2}, \frac{1}{2})$
	I		(0, 0, 0), $(\frac{1}{2}, \frac{1}{2}, \frac{1}{2})$
Trigonal	*R*	$a = b = c$ $\alpha = \beta = \gamma < 120^\circ \neq 90^\circ$	(0, 0, 0)
Hexagonal	*P*	$a = b \neq c$ $\alpha = \beta = 90^\circ$ $\gamma = 120^\circ$	(0, 0, 0)

Table III.2. The fourteen Bravais lattices. (From Sherwood, 1976, p.73).

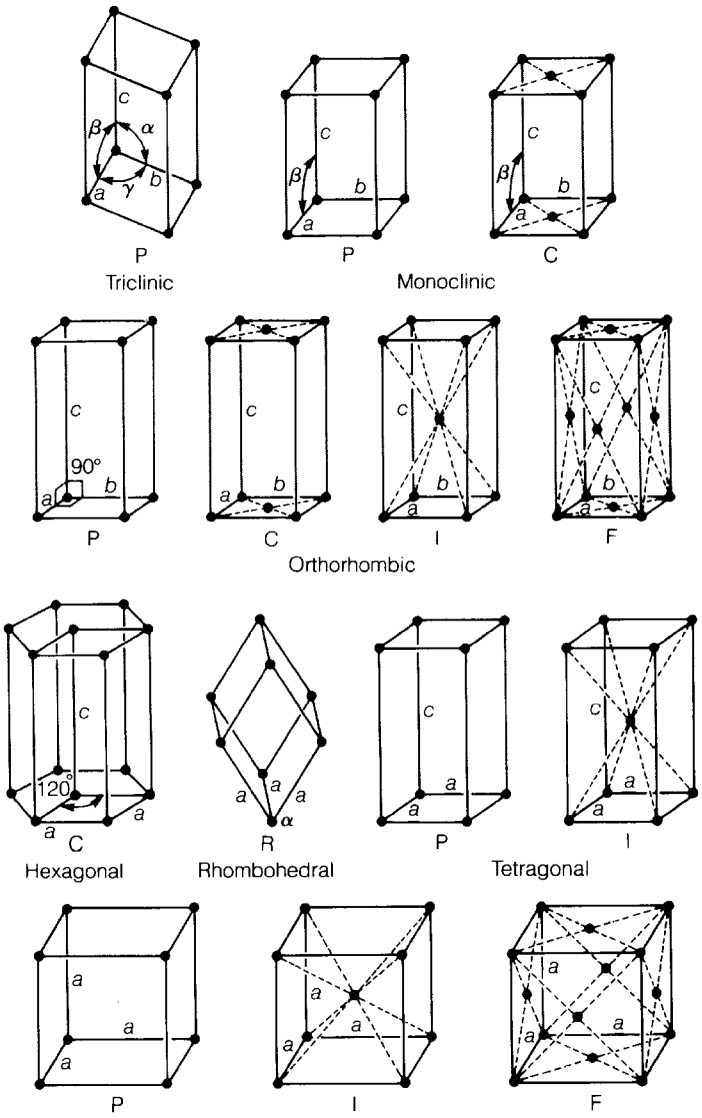

Fig. III.2. The 14 three-dimensional Bravais lattices. (From Eisenberg and Crothers, 1979, p. 790)

III.C.4. Crystal Structure

The **crystal structure** is **built by placing a motif at every lattice point**. The motif is the object that is translated, and may be asymmetric (*e.g.* a single polypeptide chain: Fig. III.3) or symmetric (*i.e.* containing two or more symmetrically arranged subunits). The crystal structure, crystal lattice, and motif are all restricted in the symmetries they can display, but biomacromolecular assemblies themselves are not restricted in the sense that they may display additional internal (**non-crystallographic**) symmetry. From this emerges the corollary that an asymmetric unit of the crystal structure may itself contain a symmetrical arrangement of identical, asymmetric molecules. The following introduction to symmetry will help clarify this.

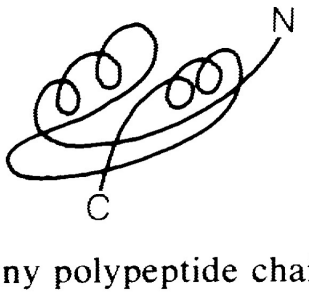

Fig. III.3. An asymmetric object. (From Eisenberg and Crothers, 1979, p. 756)

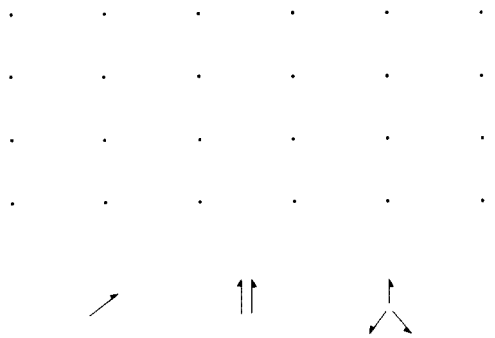

Fig. III.4. Lattices and motifs. Each of the 2D crystals depicted in Fig. III.5 may be reproduced by associating the motifs (a), (b), or (c) with the rectangular array of lattice points. (From Sherwood, 1976, p. 61)

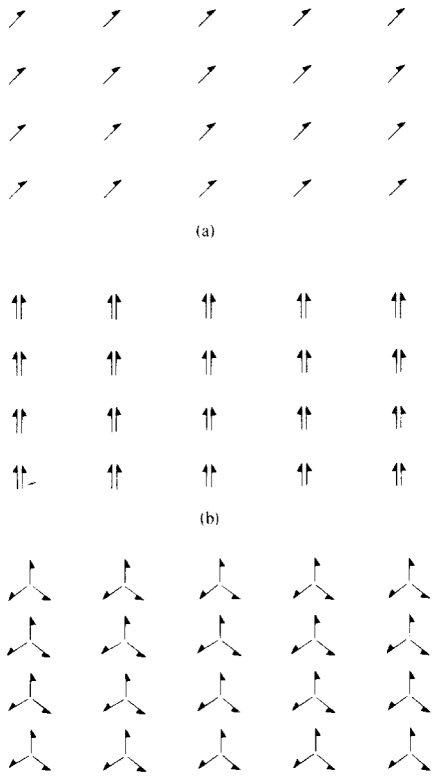

Fig. III.5. Three 2D 'crystals'. Each pattern is different, but they have the same underlying rectangular lattice as shown in Fig. III.4. (From Sherwood, 1976, p. 60)

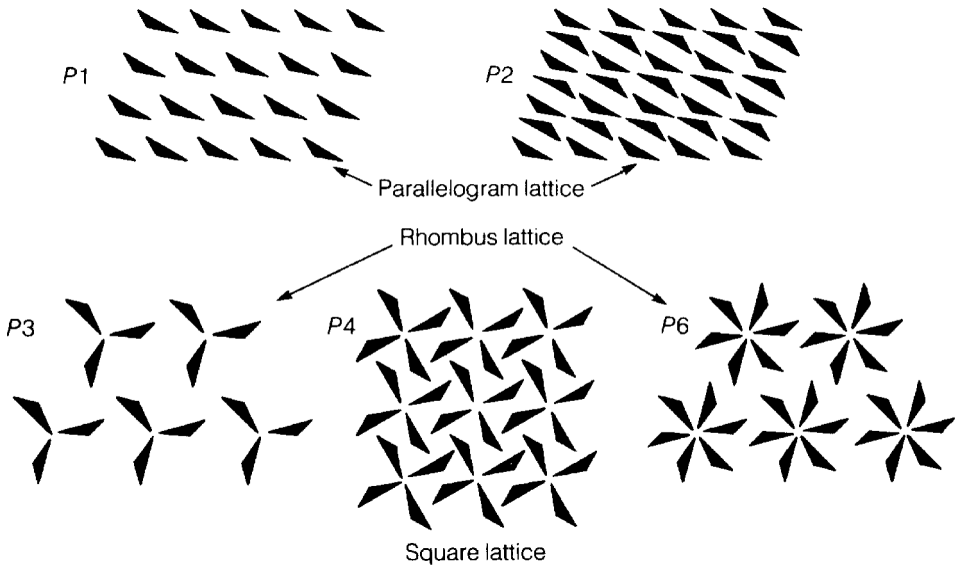

Fig. III.6. The five 2D plane groups for biological structures. The asymmetric unit is a triangle in every case; the motif is some group of triangles (1,2,3,4, or 6). (From Eisenberg and Crothers, 1979, p. 786)

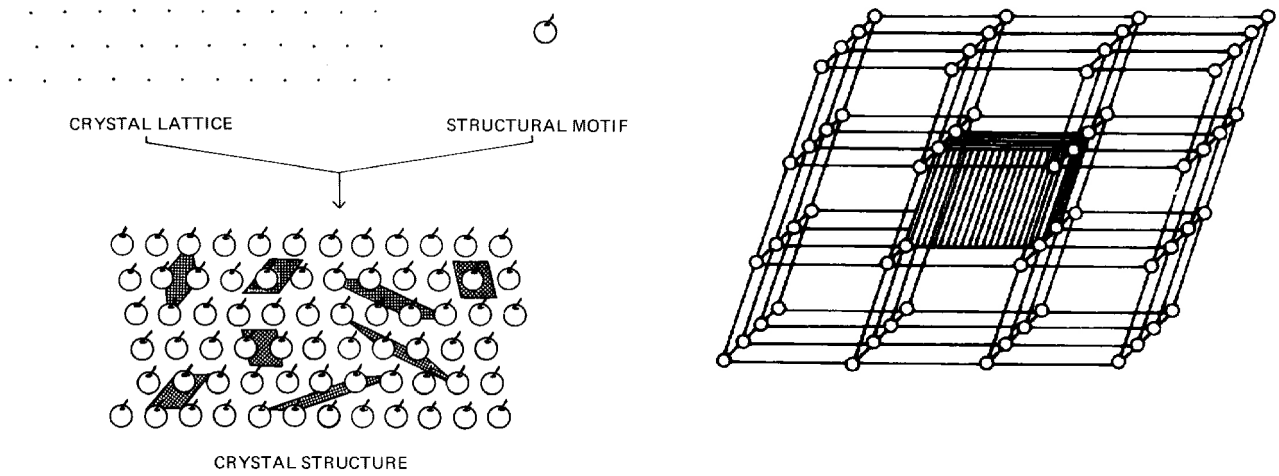

Fig. III.7. (a) Generation of a 2D "crystal structure" from a lattice and a structural motif. The replacement of each lattice point by an apple leads to a 2D structure. There are many ways in which unit cells may be chosen in a repeating pattern. Various alternative choices are shown, each having the same area despite varying shape (note that the total content of any chosen unit cell is one apple). Infinite repetition in 2D of any one of these choices for unit cell will reproduce the entire pattern. (b) Perspective view of a triclinic lattice. To see the perspective, lines that define imaginary edges of a unit cell join the lattice points. One unit cell is shaded; it could have been chosen with a different shape (but the same volume), as in the 2D example in (a). (From Glusker and Trueblood, 1972, p. 10)

III.C.5. Symmetry

Biological objects may display symmetry about a point or along a line. An object is **symmetrical** if it is indistinguishable from its initial appearance when spatially manipulated. (Again, we ignore the loss of translational symmetry at the boundary of finite, crystalline objects.)

a. Symmetry operators

There are **four types of symmetry operations** that lead to superimposition of an object on itself: **rotation, translation, reflection** and **inversion.** A **symmetry element** is a geometrical entity such as a point, line, or plane about which a symmetry operation is performed. The symmetry of any object can be described by some combination of these symmetry operations. The symmetry of any aggregate or crystal of a **biological** molecule is only described by rotation and/or translation operations. This is because, for example, biological protein molecules mainly consist of *l*-amino acids, hence, reflection or inversion symmetries are not allowed.

b. Asymmetric unit

Symmetry operations give rise to other groups of atoms (the **asymmetric unit or ASU**), which are in equivalent, general positions. The number of equivalent general positions related by the symmetry operators equals the number of ASUs in the unit cell. The ASU may be one or several molecules, or a subunit of an oligomeric molecule. If the number of asymmetric units is equal to the number of molecules in the cell, than the molecule contains no symmetry. If the number is less than the number of molecules in the cell, then the molecule contains **local symmetry** (sometimes improperly referred to as **non-crystallographic** symmetry), or symmetry that is not contained within the allowed lattice symmetries). If the number of asymmetric units is greater than the number of molecules in the cell, than the molecules must occupy special positions and possess the appropriate symmetry element of the space group (see § III.C.5.e).

c. Point groups (Symmetry about a single point)

1) Schoenflies and Herman-Mauguin point group notations

A **point group** is a collection of symmetry operations that define the symmetry about a point. Two systems of notations are used for point groups: *i*) the **S** or **Schoenflies notation** (capital letters; mainly used by spectroscopists) and *ii*) the **H-M** or **Hermann-Mauguin symbol** (an explicit

list of the symmetry elements, commonly preferred by crystallographers).

2) Types of point group symmetry operators

The four types of symmetry about a point are rotational symmetry, mirror symmetry, inversion symmetry, and improper rotations. Each of these is described below with accompanying illustrations.

Rotational symmetry (*n*): the object appears identical if rotated about an axis by $\alpha = 360/n$ degrees = $2\pi/n$ radians. The only allowed *n*-fold axes for **crystal lattices** are $n = 1,2,3,4$, and 6 since lattices must be space filling. (Figs. III.8, 9, and 12)

Fig. III.8. Two-, three-, four-, five-, and six-fold rotational symmetries. (From Bernal, 1972, pp.45,48,50,35,

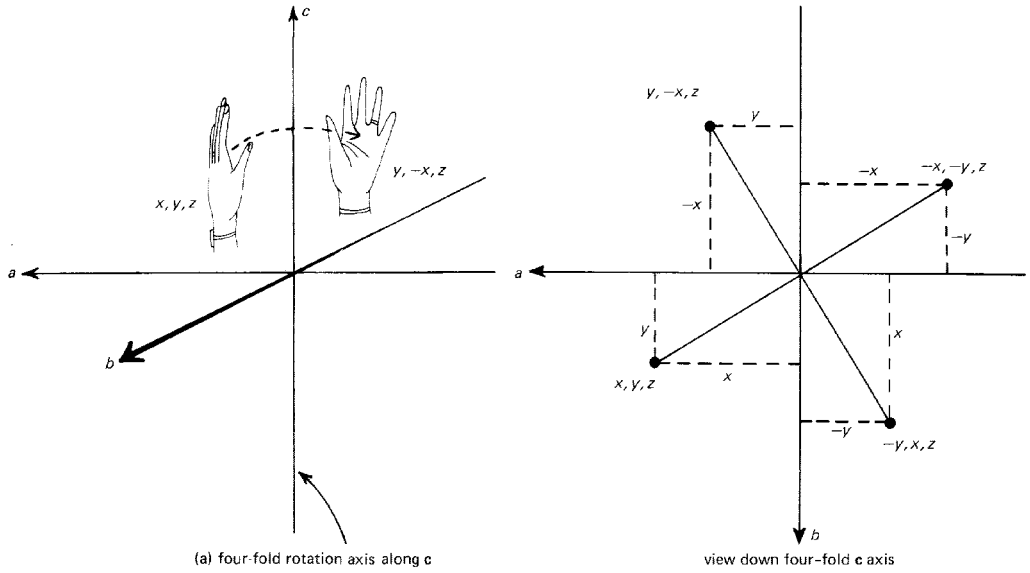

Fig. III.9. A four-fold rotation axis, parallel to **c** and through the origin of a tetragonal unit cell (a=b), moves a point at *x, y, z* to a point at (*y, -x, z*) by a rotation of 90 about the axis. The sketch on the right shows four equivalent points resulting from successive rotations. (From Glusker and Trueblood, 1972, p. 72)

Mirror (reflection) symmetry (*m*): each point in the object is converted to an identical point by projecting through a mirror plane and extending an equal distance beyond this plane. (Figs. III.10 and III.11)

Inversion symmetry (*i*): each point in the object is converted to an identical point by projecting through a common center and extending an equal distance beyond this center. Objects with ***i*** symmetry are said to be **centrosymmetric.** (Fig. III.10)

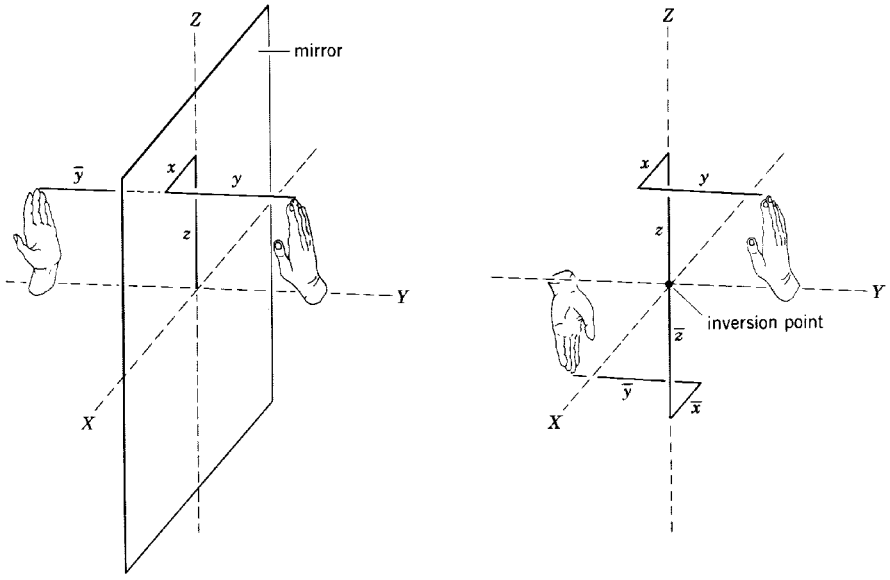

Fig. III.10. (Left) A mirror symmetry operation. (Right) An inversion symmetry operation. (From Buerger, 1971, p. 8)

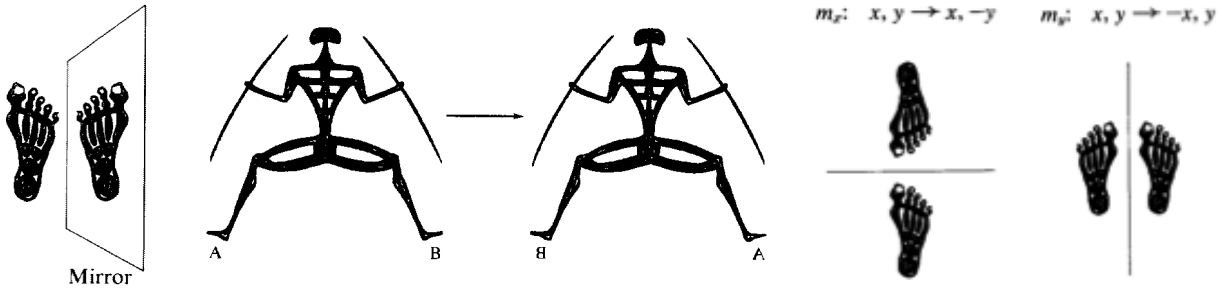

Fig. III.11. Additional examples of mirror symmetry operations. (Right) m_y and m_x. (From Bernal, 1972, pp. 26, 27, and 34)

Improper rotations: rotations followed by ***m*** or ***i***. These include the **rotoinversion** (***n*** followed by ***i***) and **rotoreflection** (***n*** followed by ***m***). The only **inversion axes** allowed for crystal lattices are $\bar{1}$, $\bar{2}$, $\bar{3}$, $\bar{4}$, $\bar{6}$. (Figs. III.12 and III.13)

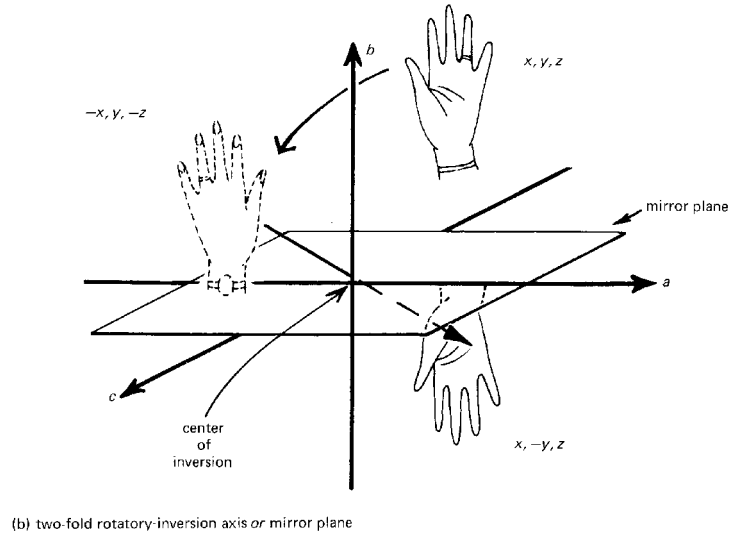

(b) two-fold rotatory-inversion axis *or* mirror plane

Fig. III.12. The operation $\bar{2}$, a two-fold rotary-inversion axis parallel to **b** and through the origin, converts a point at *x, y, z* to a point at *x, -y, z.* This is the result of, first, a two-fold rotation about an axis through the origin and parallel to **b** (*x, y, z* to *-x, y, -z*) and then an inversion about the origin (*-x, y, -z* to *x, -y, z*). This is the same as the effect of a mirror plane perpendicular to the **b** axis. Note that a right hand has been converted to a left hand. (From Glusker and Trueblood, 1972, p. 72)

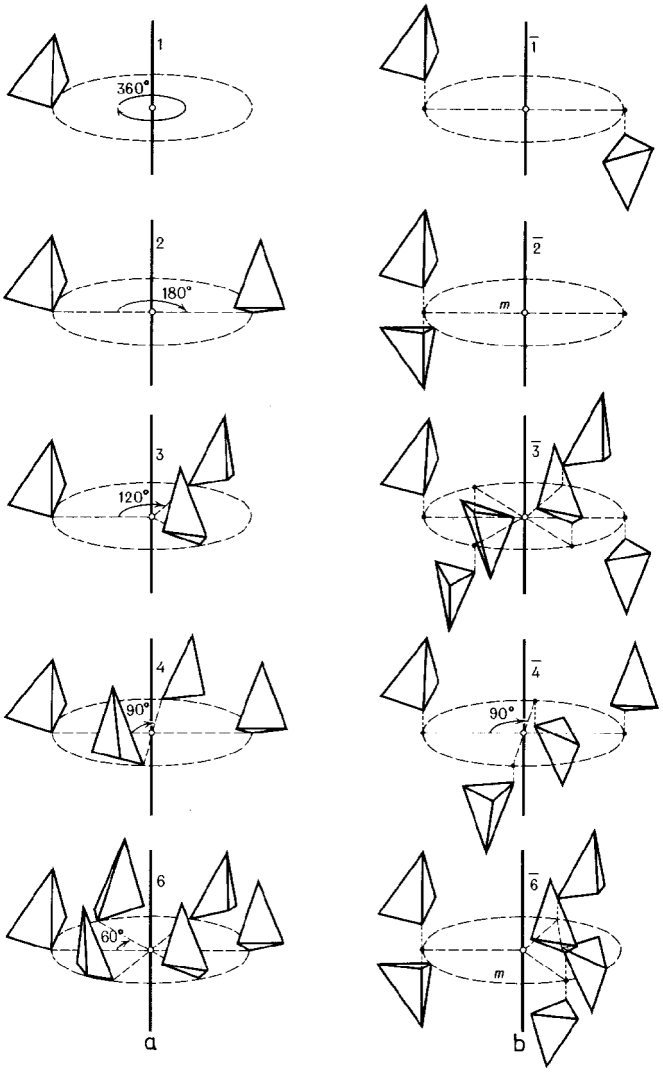

Fig. III.13. Crystallographic rotation (a) and inversion-rotation (b) symmetry axes and their action on an asymmetric figure - a tetrahedron. (From Vainshtein, 1981, p. 67)

3) Types of point groups

Cyclic, dihedral, and cubic (tetrahedral, octahedral and icosahedral) point groups define the collection of symmetry operations about a point. Klug (1969) and others (*e.g.* Wilson, 1966; Glusker and Trueblood, 1972; Eisenberg and Crothers, 1979; Bernal, Hamilton and Ricci, 1972) describe this and other aspects of symmetry in detail.

Cyclic point groups

These contain a single *n*-fold axis of rotation, where ***n*** can be any positive integer and also may contain one or more planes of reflection (Fig. III.8 and III.15, next page). Point groups that contain only an *n*-fold axis of rotation are given the symbol ***n*** in the **H-M** system and C_n in the **S** system (***C*** stands for cyclic). For example, the double-disk structure of tobacco mosaic virus (TMV) stacked disk aggregates contains 34 subunits (polypeptide chains) arranged with C_{17} symmetry (**S** notation) (Fig. III.14). Non-biological molecules can also have mirror planes of symmetry either parallel (*e.g.* ***nm*** or ***nmm*** in the **H-M** notation or C_{nv} in the **S** notation where *v* stands for vertical) or perpendicular (e.g. ***n/m*** in the **H-M** notation or C_{nh} in the **S** notation where *h* stands for horizontal) to the *n*-fold axis of symmetry.

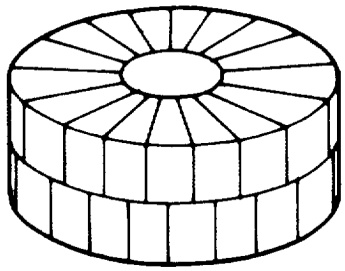

Fig. III.14. The TMV stacked disk structure with C_{17} symmetry. (From Eisenberg and Crothers, 1979, p.757)

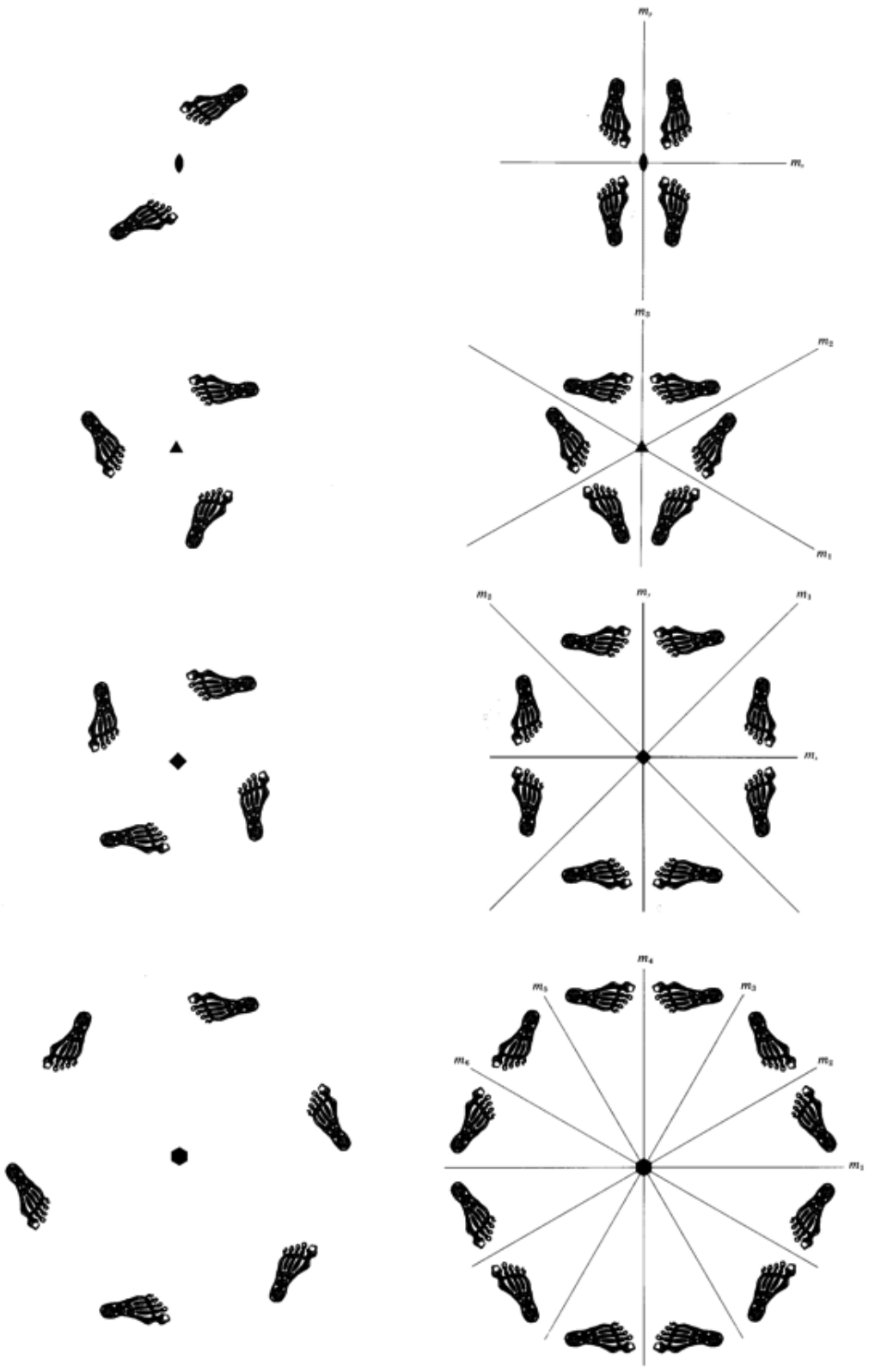

Fig. III.15. Examples of cyclic point groups. (From left to right and top to bottom) 2, 2mm, 3, 3m, 4, 4mm, 6, and 6mm (From Bernal, 1972, pp. 45, and 47-53)

Dihedral point groups

Dihedral point groups have axes of rotation at right angles to each other. These point groups consist of an ***n*-fold axis perpendicular to *n* 2-fold axes.** Most oligomeric enzymes display dihedral symmetry (Matthews and Bernhard, 1973). For example, the enzyme ribulose bisphosphate carboxylase/oxygenase (RuBisCO) has D_4 symmetry (**422** in **H-M** notation). The number of asymmetric units in the point group D_n is $2n$, thus RuBisCO has eight asymmetric units. In this particular enzyme, each asymmetric unit contains two polypeptide chains: a large (~55 kD) catalytic subunit and a small (~15 kD) subunit whose function remains enigmatic.

Cubic point groups

The essential characteristic of the three cubic point groups is **four 3-fold axes arranged as the four body diagonals** (lines connecting opposite corners) **of a cube.** The three cubic point groups are *T* (tetrahedral = **23** in **H-M** notation), *O* (octahedral = **432**) and *I* (icosahedral = **532**) (Fig. III.16). The tetrahedral point group contains 12 asymmetric units. Aspartate-ß-decarboxylase is presumed to display this point group symmetry (Eisenberg and Crothers, 1979). Dihydrolipoyl transsuccinylase contains 24 asymmetric subunits arranged with octahedral (**432**) symmetry. There are a large number of plant, animal, and bacterial viruses, each containing 60 asymmetric units, which display icosahedral (**532**) symmetry (Fig. III.17). In most instances, these spherical viruses contain a multiple of 60 copies of chemically identical or distinct protein or glycoprotein subunits. In those cases where the asymmetric unit contains more than one "subunit", not all subunits are equivalently arranged. Instead they occupy **quasi-equivalent** positions.

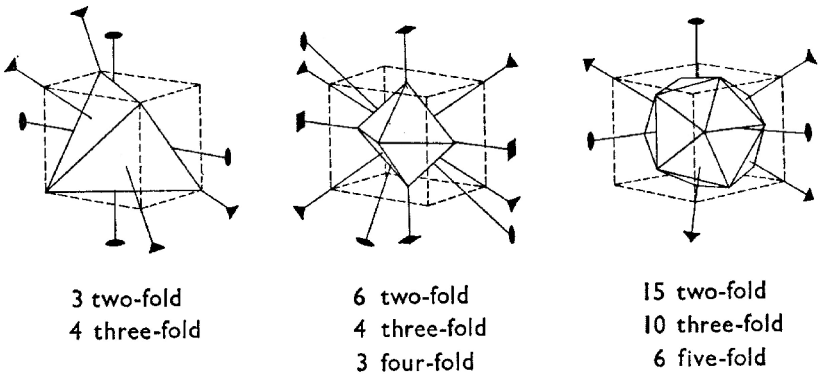

Fig. III.16. Diagrams showing (a) a tetrahedron, (b) an octahedron and (c) an icosahedron, inscribed in a cube. The number and type of rotation axes of the tetrahedron, octahedron and icosahedron are also listed, and some of these are shown in the diagrams. (From Wilson, 1966, p.126)

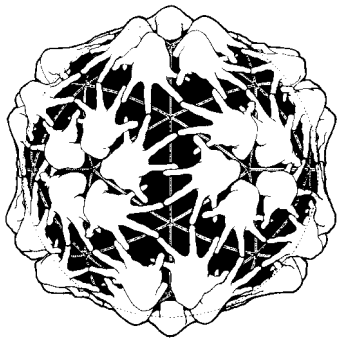

Fig. III.17. Schematic drawing of an icosahedral virus (532 symmetry) that consists of 60 hands, all in identical environments. (From Eisenberg and Crothers, 1979, p. 767; Drawing by D. L. D. Caspar)

4) Lattice restrictions and non-crystallographic symmetry

The **crystal structure** and **crystal lattice may only contain one-, two-, three-, four-, or six-fold rotational symmetry axes** (because the crystal lattice must be space filling) though the **motif** can have additional symmetries. For example, the 34 subunits in the disc structure of TMV are arranged about a 17-fold axis of rotation (Fig. III.14). The TMV disc forms true 3D crystals and has been studied by X-ray crystallography. In the crystal, the disc occupies a general position in the unit cell, and therefore displays **non-crystallographic** symmetry. Many of the small, spherical viruses are icosahedral (cubic point group) and they contain symmetry elements compatible with allowed lattice symmetries, and crystallize and display crystallographic as well as non-crystallographic symmetry.

d. Translational symmetry (Symmetry along a line)

1) Repetition in one dimension

Translation is the symmetry operation in which an object is shifted a given distance, say *t*, in a given direction, say the *x* direction, as illustrated in Fig. III.18 (1D crystal of right feet). The group of feet can be superimposed on itself if it is shifted in the *x* direction by the translation *t*. In this 1D

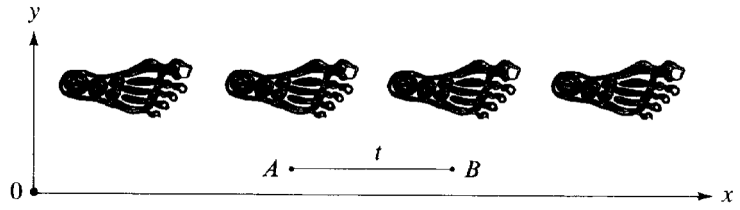

Fig. III.18. A one-dimensional 'crystal' of right feet. (From Bernal, 1972, p.27)

crystal, each foot occupies one unit cell and the distance *t* is the unit cell edge of the crystal.

2) Screw axes

A **screw axis** combines translation and rotation operations to produce a structure with helical symmetry (Figs. III.19-21). Screw axes are symmetry elements of crystals that are helices with an **integral** number of asymmetric units per turn of the helix. An n_m screw axis combines a **rotation of $2\pi/n$ radians about an axis, followed by a translation of m/n of the repeat distance (unit cell edge).** The screw axes found in crystals include 2_1, 3_1, 3_2, 4_1, 4_2, 4_3, 6_1, 6_2, 6_3, 6_4, and 6_5. A crystal lattice only accommodates an integral number of asymmetric units per turn of the helix, although this need not apply to isolated helices in general.

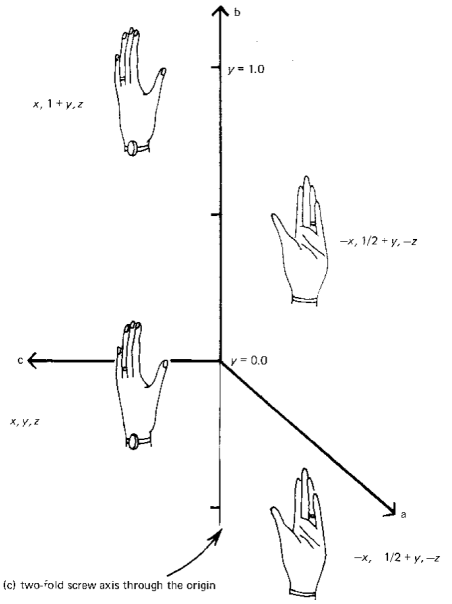

Fig. III.19. A two-fold screw axis, 2_1, parallel to **b** and through the origin, which combines both a two-fold rotation (*x, y, z* to *-x, y, -z*) and a translation of **b**/2 (*-x, y, -z* to *-x, 1/2+y, -z*). A second screw operation will convert the point *-x, 1/2+y, -z* to *x, 1+y, z*, which is the equivalent of *x, y, z* in the next unit cell along **b**. Note that the left hand is *never* converted to a right hand. (From Glusker and Trueblood, 1972, p. 73)

Aggregates such as actin thin filaments, microtubules, and the TMV particle (*i.e.* the virion, not the stacked disk shown in Fig. III.14) are helical structures and all display symmetry along a line. For example, one turn of the basic helix of the TMV rod contains 16.33 protein subunits (Fig. III.22). The true repeat in the structure is, therefore, three turns of the basic helix, which contains 49 subunits altogether. Most helical biological aggregates do not form 3D crystals suitable for diffraction studies, not because of strict symmetry constraints (they could occupy non-crystallographic positions), but rather as a consequence of their shape and large size.

e. Plane groups and space groups

The symmetry of a structure is described by a **plane group** if it is 2D or by a **space group** if it is 3D. All possible crystal symmetries are generated by combining all types of lattice symmetries with all types of motif symmetries. If the internal structure of the crystal is considered, additional symmetry exists due to the presence of screw axis and glide plane symmetries. This leads to **17 possible plane groups** in two-dimensions and **230 space groups** in three-dimensions. Thus, there are only 17 ways in which to generate a two-dimensional regular pattern from a motif associated with a two-dimensional lattice and 230 ways in which to generate a 3D regular pattern from a motif associated with a 3D lattice. Volume I of the International Tables for X-ray Crystallography (Henry and Lonsdale, 1969) provides descriptions and formulas for all the plane groups and space groups.

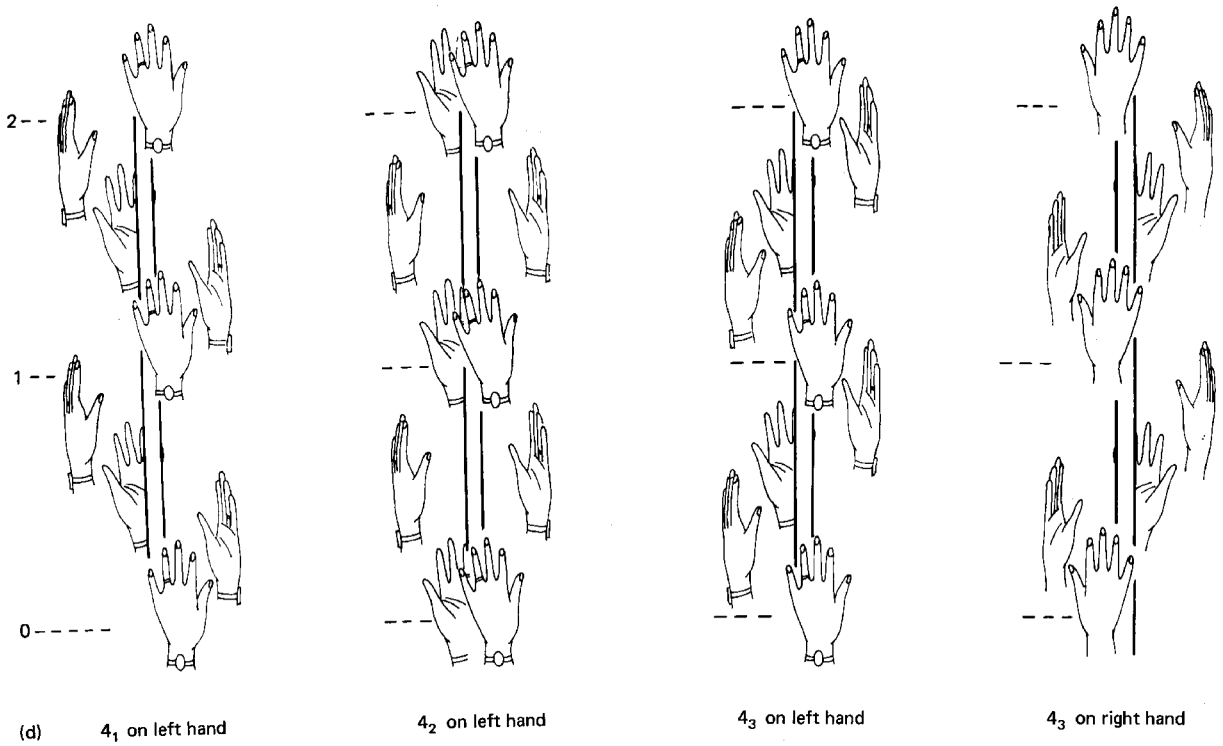

Fig. III.20. Some crystallographic four-fold screw axes showing two identical points for each. Note that the effect of 4_1 on a left hand is the mirror image of the effect of 4_3 on a right hand. The right hand has been moved slightly to make this relation obvious. (From Glusker and Trueblood, 1972, pp. 74-75)

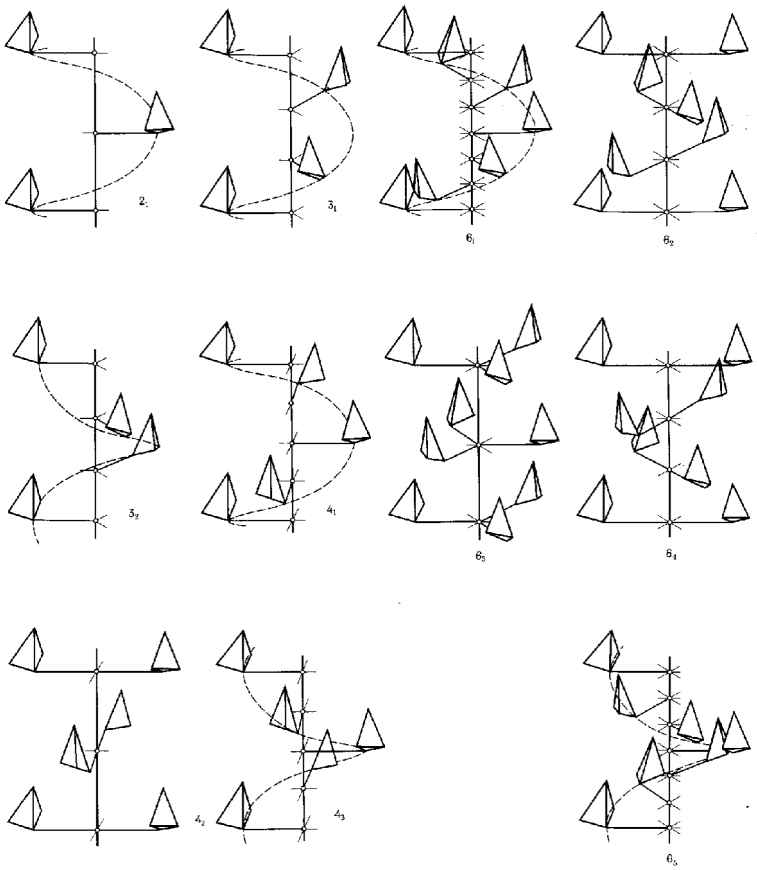

Fig. III.21. Crystallographic screw axes and their action on an asymmetric tetrahedron. (From Vainshtein, 1981, p. 69)

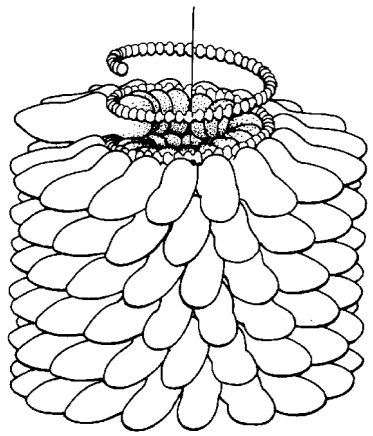

Fig. III.22. Drawing of part of the helical structure of tobacco mosaic virus. Each shoe-shaped protein subunit is bound to three RNA nucleotides. Part of the RNA chain is shown stripped of its protein subunits in a configuration it could not maintain without them. Each turn of 16.3 protein subunits is closely related to the disk structure shown in Fig. III.14.. (From Eisenberg and Crothers, 1979, p. 782)

Only five plane groups and **65 space groups** are compatible with biological (i.e. enantiomorphic) structures. Some examples of 2D plane groups are shown in figures III.6 and III.23. The initial stage of most X-ray crystallographic structure analyses involves the space group determination. When this is known, the number of asymmetric units in the unit cell is also known. Thus, it is often possible to learn the packing and number of molecules within the unit cell, and prove if the molecules are symmetric. Symmetry operations in the unit cell give rise to systematic absences in the diffraction patterns. The distribution of absences in the diffraction patterns often proves useful for determining the correct plane or space group. The number of molecules per unit cell or per asymmetric unit is usually deduced from estimates of the molecular weight and measurements of the crystal density and unit cell volume. In many instances, image processing of electron micrographs of periodic biological specimens provides an objective means for determining or verifying these types of structural information.

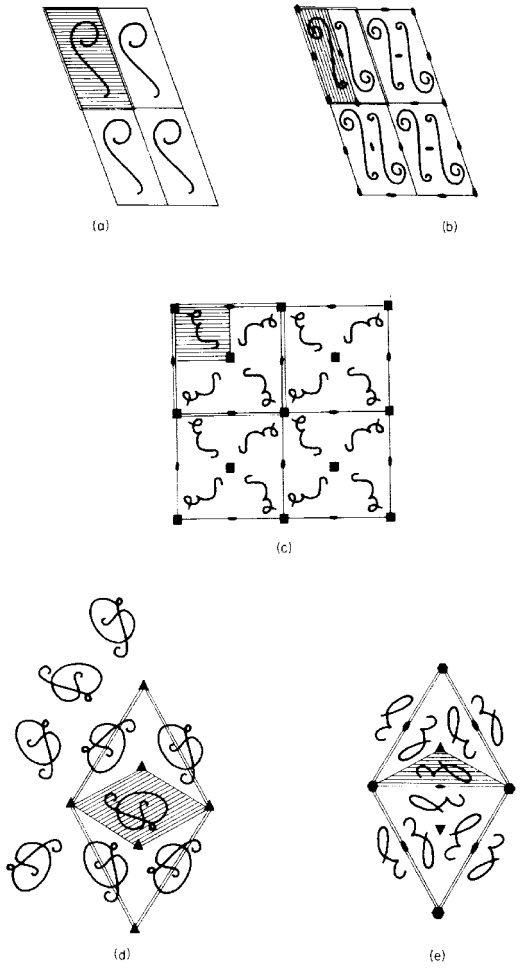

Fig. III.23. Rotational symmetry elements (a) 1 (b) 2 (c) 4 (d) 3 and (e) 62. A single unit cell is outlined by a double set of lines. Other unit cells are shown with single lines. The asymmetric unit is shown shaded. (From Blundell and Johnson, 1976, p. 87)

Placing a motif at every point of a lattice generates a periodic structure. The **lattice is a rule for translation** and the **motif is the object that is translated**. Figures III.18 and III.24-27 illustrate examples of both one- and two-dimensional crystal structures. Notice that the motif does not always have to be an asymmetric object such as a right foot. In biological crystals, the motif often has the symmetry of one of the point groups or one of the screw axes. In such cases the periodic structure contains translational symmetry plus rotational (or reflection or inversion in some, mostly small biological molecules) symmetry. The periodic structure can be thought of as being built up in two steps. First a motif is generated from the asymmetric unit by the symmetry operations of the point group. Second, the structure is generated from the motif by the translational symmetry operations of the lattice:

$$Asymmetric\ Unit \xrightarrow[\substack{point-group\\ symmetry}]{} Motif \xrightarrow[lattice\ symmetry]{} Structure$$

Glide plane symmetry is produced by a translation followed by a mirror operation or vice versa (Figs. III.28-III.29). Biological molecules do not, in general, display glide plane symmetries because they do not exist in enantiomorphic pairs. However, note that biological molecules (or crystals) when viewed in two-dimensions (*i.e.* in projection) **can** display mirror symmetry.

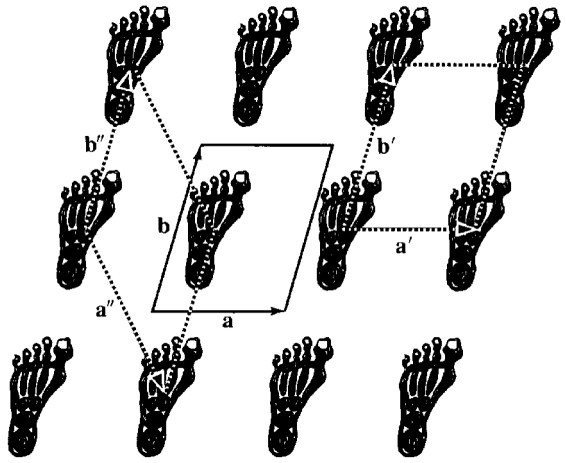

Fig. III.24. Plane group symmetry P1. (From Bernal, 1972, p. 58)

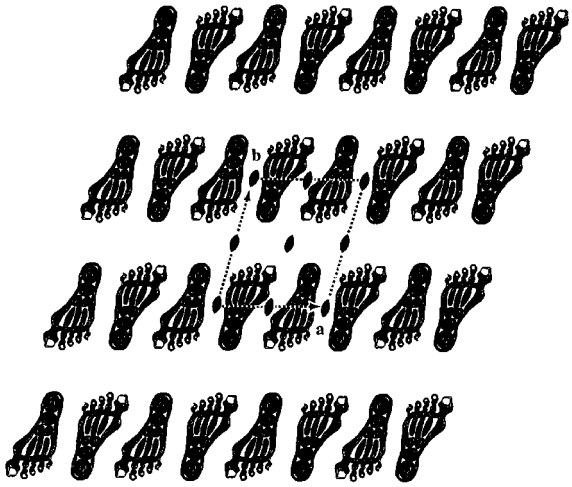

Fig. III.25. Plane group symmetry P2. (From Bernal, 1972, p. 59)

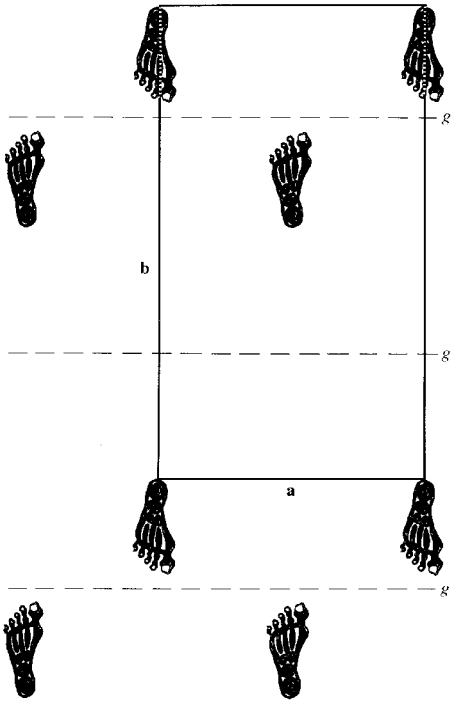

Fig. III.26. Plane group symmetry Pg. (From Bernal, 1972, p. 61)

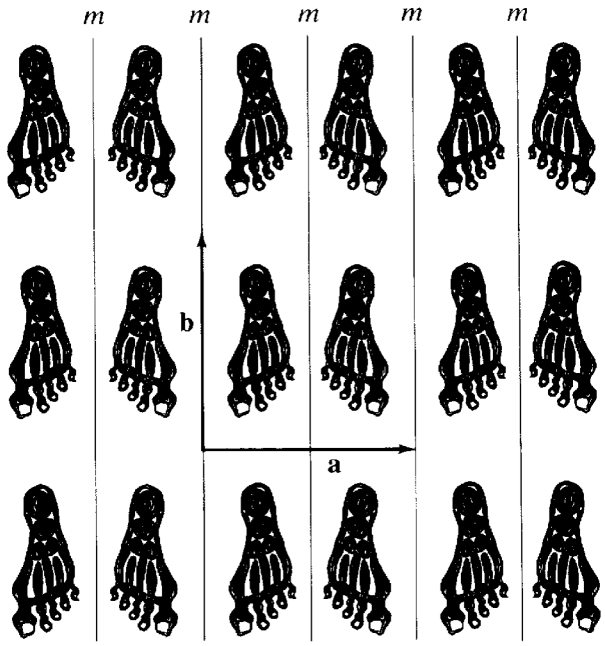

Fig. III.27. Plane group symmetry Pm. (From Bernal, 1972, p. 60)

Fig. III.28. A glide symmetry operation. (From Buerger, 1971, p. 8)

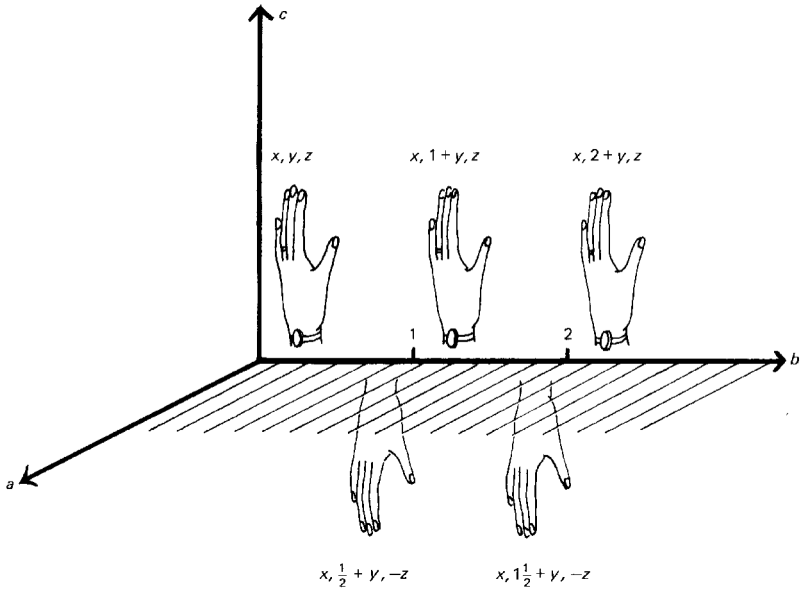

Fig. III.29. A b-glide plane normal to **c** and through the origin involves a translation of **b**/2 and a reflection in a plane normal to **c**. It converts a point at *x, y, z* to one at *x, y+1/2, -z*. Note that left hands ARE converted to right hands, and *vice versa*. (From Glusker and Trueblood, 1972, p. 74)

f. Examples of symmetrical biological molecules

1) Helical symmetry

Actin filament	Bacterial flagella
Chromatin fibers	Neurotubules
Bacterial pili	Sickle cell hemoglobin fibers
Tobacco mosaic virus	Enzyme aggregates (*e.g.* catalase tubes)

T4 bacteriophage sheath (extended or contracted configuration)

Acetylcholine receptor tubes

2) Point group symmetry

MOLECULE/AGGREGATE	S	H-M	# ASU
Asymmetric aggregates: *e.g.* ribosome (monomer)	C_1	1	1
Fibrous molecules: *e.g.* fibrinogen	C_2	2	2
Enzymes:			
Lactate dehydrogenase	D_2	222	4
Catalase	D_2	222	4
Aspartate transcarbamylase	D_3	32	6
Ribulose bisphosphate carboxylase/oxygenase	D_4	422	8
Glutamine synthetase	D_6	622	12
Asparate-β-decarboxylase	T	23	12
Dihydrolipoyl transsuccinylase	O	432	24
Spherical viruses: *e.g.* polyoma, polio, rhino, tomato bushy stunt, human wart, rotavirus, and hundreds more.	I	532	60

3) **Plane group symmetry** (2D crystals)
   Aquaporin membrane
   Bacterial cell walls (*e.g. Bacillus brevis* T layer)
   Bladder luminal membrane
   Gap junctions
   Purple membrane

4) **Space group symmetry** (3D crystals)
   Various intracellular inclusions
   Various *in vitro* grown crystals suitable for X-ray crystallography

III.C.6. Diffraction

Diffraction methods, including X-ray, neutron, electron, and optical diffraction, provide powerful ways to study molecular structure. The ultimate goal is to understand the chemical properties of molecules by determining their atomic structure (*i.e.* the types of chemical bonds - ionic, covalent, or hydrogen-, their lengths and angles, Van der Waals radii, rotations about single bonds, etc.). Presently, only X-ray and neutron diffraction techniques are routinely capable of revealing the arrangement of atoms in molecular structures. In 1912 von Laue predicted that X-rays should diffract from crystals like light from a diffraction grating. Friedrich and Knipping later verified this prediction experimentally. W. L. Bragg developed the concept of diffraction from crystal planes (§ III.C.6.e) and that the diffraction pattern could be used to reveal atomic positions in crystals (See also § I.F.1.a and Fig. I.148). The physical principles of X-ray diffraction form the fundamental basis of Fourier image processing techniques.

a. Introduction to diffraction theory (see also pp.10-14, § I.A.3.c for review)

Diffraction is the non-linear propagation of electromagnetic radiation and occurs when an object scatters the incident radiation. The radiation scattered from different portions of the object interfere both constructively and destructively, producing a diffraction pattern that can be recorded on a photographic emulsion. In an electron microscope, electrons are scattered both by the electrons (inelastic scatter) and nuclei (elastic scatter) of the specimen atoms (§ I.C.1). X-rays are scattered by the electrons of atoms.

A characteristic of diffraction is that ***each point*** in the diffraction pattern arises from interference of rays scattered from ***all irradiated portions*** of the object. Structure determination by diffraction methods involves measuring or calculating the **structure factor** (*F*) at many or all points of the diffraction pattern. **Two quantities**, **amplitude** and **phase,** describe each **F. Amplitude,** the strength of interference at a particular point, is proportional to the square root of the intensity in the recorded pattern (photographic film does not record the scattered amplitude, but rather the intensity, which is proportional to the amplitude squared). **Phase** is the relative time of arrival of the scattered radiation (wave) at a particular point (*e.g.* photographic film), and this information is lost when the **diffraction** pattern is recorded. Phases cannot, therefore, be measured directly from X-ray diffraction photographs. A major concern of structure determination using X-ray crystallography is the regeneration of the lost phase information. Several techniques, including the heavy atom, isomorphous replacement and molecular replacement methods were devised to solve the so-called **"phase problem"** (see *e.g.* any general textbook on crystallography such as: Eisenberg and Crothers, 1979; Glusker and Trueblood, 1972; Holmes and Blow, 1965; Wilson 1966).

X-ray phases could be obtained if it were possible to rediffract (focus) the scattered rays with a lens to form an image. Fortunately, we can **directly** visualize structure in electron and light microscopes because electrons and visible photons scattered by specimens can be focused with lenses to form images. In the absence of "noise", an image might be considered to contain structural information (amplitudes and phases) in directly interpretable form. A major advantage of image processing is that it provides an objective means to extract reliable structural information from noisy images.

b. The Fourier transform

Knowledge of Fourier transforms is essential for understanding the principles of diffraction methods. The **Fourier transform**, named after the nineteenth century, French mathematician, Joseph Fourier, mathematically describes the distribution of amplitude and phase in different directions, for all possible directions of the beam incident on the object.

The Fourier transform of an object is a particular kind of weighted integral of the object. In one-dimension, the Fourier transform is mathematically expressed in the following way:

$$F(X) = \int_{-\infty}^{\infty} \rho(x) e^{(2\pi i x X)} dx \qquad \text{(III.C.6.1)}$$

$F(X)$ is called the scattering function and $\rho(x)$ is called the electron density function. The integration is over **all** values x in the structure. For the case in which there is a discrete summation over **sampled** points in the structure the above expression becomes:

$$F(X) = \sum_{x} \rho(x) e^{(2\pi i x X)} \qquad \text{(III.C.6.2)}$$

F is a shorthand notation for the Fourier transform of ρ, *i.e.* $F = T(\rho)$, where *"T"* represents the **forward** Fourier transformation operation.

A property of Fourier transforms is that the **inverse relationship** holds, namely:

$$\rho(x) = \int_{-\infty}^{\infty} F(X) e^{(-2\pi i x X)} dX \qquad \text{(III.C.6.3)}$$

Thus, ρ is the **inverse transform** of F, *i.e.* $\rho = T^{-1}(F)$, where "T^{-1}" signifies an **inverse** Fourier transformation operation.

Thus, $$\rho = T^{-1}(T(\rho)) \qquad \text{(III.C.6.4)}$$

This expression emphasizes an important property of the Fourier transform, called the **inversion theorem:** the Fourier transform of the Fourier transform of an object is the original object. This theorem is analogous to Abbe's treatment of image formation, which is considered to be a double-diffraction process (see § III.C.6.d later). The **recorded** diffraction pattern of an object is the **square** of the Fourier transform of that object.

c. Fourier synthesis

Joseph Fourier also showed that any **periodic function** could be mathematically represented by a summation of a series of sinusoidal waves. In one-dimension, the Fourier synthesis can be expressed in the following way:

$$\rho(x) = \sum_{n=-\infty}^{\infty} A_n \cos(2\pi n x / a) \qquad \text{(III.C.6.5)}$$

where
- $\rho(x)$ = one-dimensional density function
- x = coordinate of a point in the object
- a = repeat distance
- A_n = Fourier coefficient (amplitude term) for wave number n
- n = wave number (frequency) or cycles per repeat distance a
- $(2\pi nx/a)$ = phase term (position of wave with respect to a fixed origin point in the repeating structure)

A 1D periodic function and the relative amplitudes and phases of the six component waves are shown in Fig. III.30. **Wave number** refers to the number of complete cycles of each wave per repeat distance. Mathematical combination of the waves to produce the periodic function is called **Fourier synthesis,** and the opposite process, decomposition of the function into its component waves, is called **Fourier analysis** (Figs. III.30-32). The latter is formally equivalent to analyzing

the sound wave harmonics of a musical instrument. The analogy between music and structure can be represented as follows:

$$\text{tone} = \Sigma \text{ harmonics}$$
$$\text{structure} = \Sigma \text{ structure factors}$$

Diffraction methods provide a direct way to display the decomposition of a function into component waves (frequencies), and for this reason, diffraction is often called **spatial frequency spectrum analysis** or **harmonic analysis.**

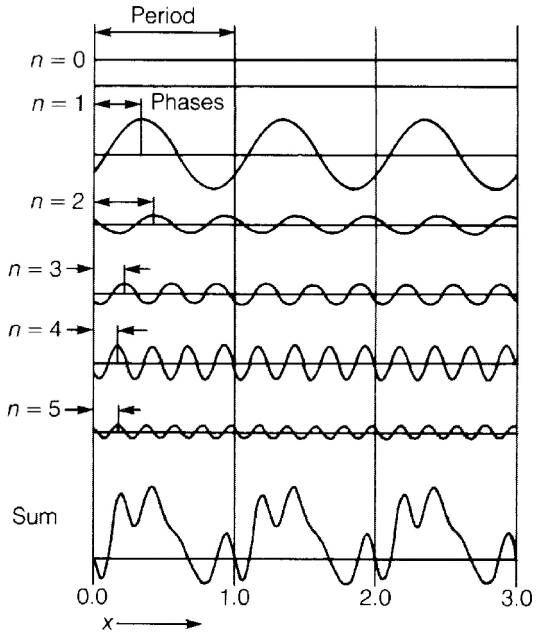

Fig. III.30. Superposition of sinusoidal waves to yield a periodic function. The wave numbers and phases of the component waves are shown. (From Eisenberg and Crothers, 1979, p. 828)

d. Image formation as a double-diffraction process

Image formation, according to Abbe's theory, is a two-stage, double-diffraction process (Figs. III.33-35). That is, an **image** is the diffraction pattern of the diffraction pattern of an object. With an "ideal" lens system, an image precisely depicts every detail present in the object. In the first stage of image formation, a collimated (parallel) beam of rays incident on the object is scattered and the interference pattern (Fraunhofer diffraction pattern) is brought to focus at the back focal plane of the lens. This stage is sometimes referred to as the forward Fourier transformation. The **intensity distribution** of the **recorded diffraction pattern** of an object is proportional to the square of the Fourier transform of the object. Although they are not equivalent, the terms, transform and diffraction pattern, are often used interchangeably.

A lens, essential for image formation, also acts to focus the diffraction pattern at a finite distance from the object (at the back focal plane of the lens if the object is illuminated by a coherent beam of radiation). If the lens is removed from behind the object, no image forms, but instead **Fresnel** diffraction patterns form at finite distances from the object (see Fig.I.10 on p.11 of § I.A.3.c) and the **Fraunhofer** diffraction pattern forms at infinity (or large distance relative to the object size or wavelength of radiation used). In X-ray diffraction experiments, where there is no lens to focus the X-rays, a Fraunhofer diffraction pattern is generally photographed about 50 to 150 mm behind the specimen. This distance is large relative to the size of the diffracting objects (*i.e.* unit cells about 10-50 nm in dimension) and the wavelength of the incident radiation (usually 0.154 nm).

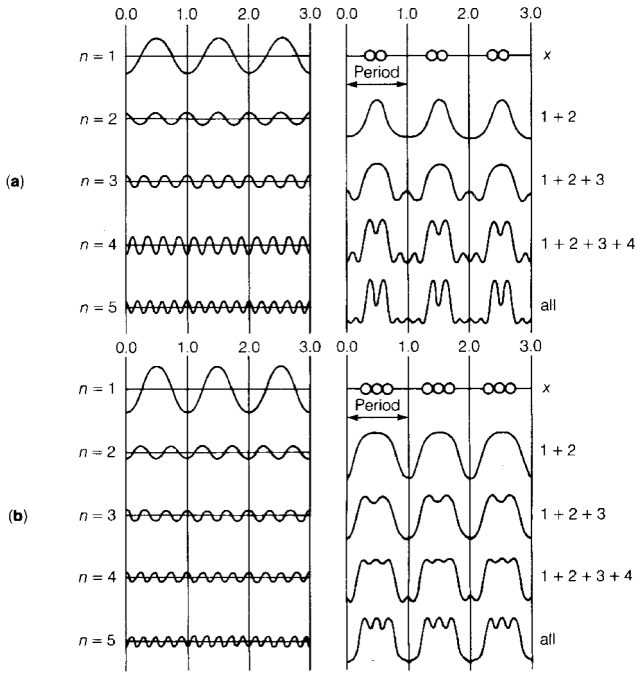

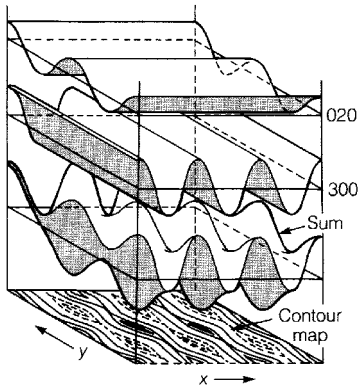

Fig. III.31. (Left, upper) Representation of the electron density of a 1D "crystal" by a superposition of waves. The crystal is formed by a periodic repetition of a diatomic molecule, as shown at the top of the right hand column. The component waves, each with proper phase and amplitude, are on the left. The curves on the right show the successive superposition of the five waves on the left. (Left, lower) Representation of another 1D crystal, this one containing a triatomic molecule. Note that this crystal is built up from the same waves as the crystal of (a); only the amplitudes and phases have been changed. (Top, right) The summation of 2D waves to produce a 2D "electron density". (From Eisenberg and Crothers, 1979, pp. 829-830)

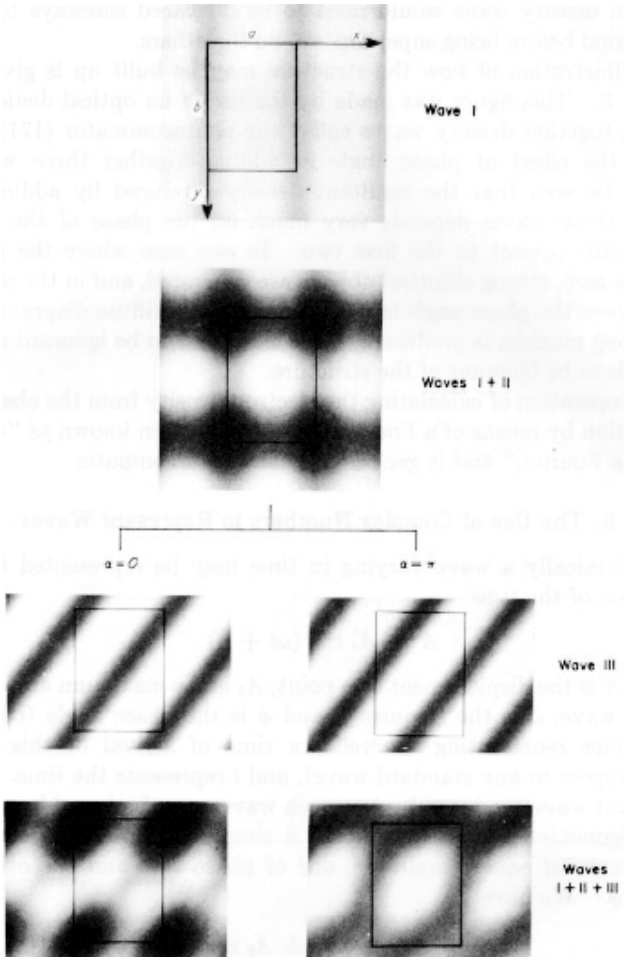

Fig. III.32. Each diffraction spot arises from an electron density wave in the crystal. If the amplitude and phase of each reciprocal lattice point are known, the crystal structure can be synthesized by adding together the appropriate electron density waves. A pictorial example of this is shown at the left. Note that the phase angle of the third wave added has considerable effect on the type of structure produced. (From Holmes and Blow, 1965, p. 131)

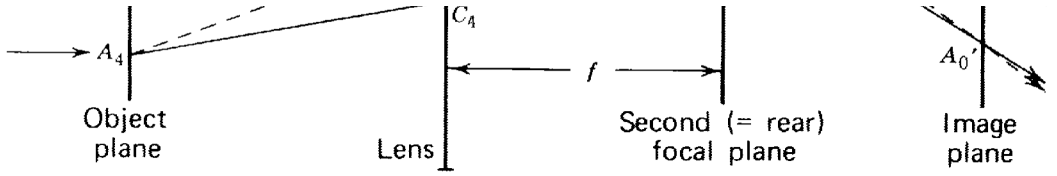

The **second stage of image formation** occurs when the scattered radiation passes beyond the back focal plane of the lens and interferes (recombines) to form an image (Figs. III.33-35). This is the **back or inverse Fourier transformation stage.** Note that the image cannot exactly represent the object because some scattered rays never enter the lens and cannot be focused at the image plane to recover all information from the object. Typical specimens for diffraction experiments are predominantly transparent to the radiation, that is, most rays pass straight through the object without being scattered.

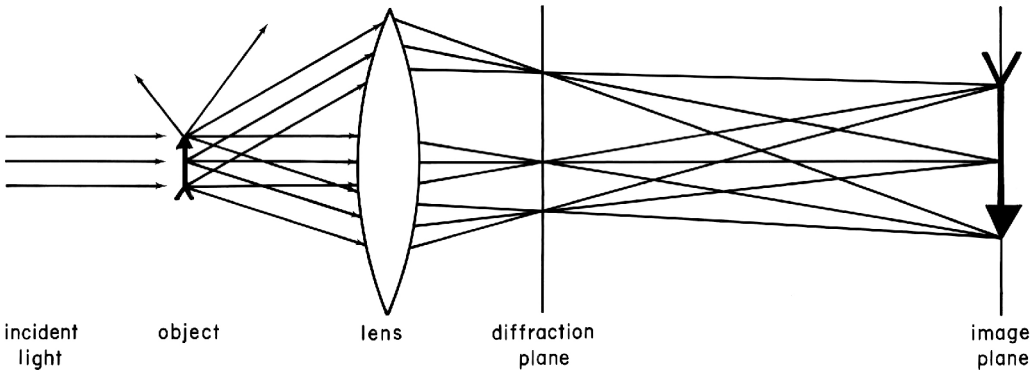

Fig. III.33. Image formation in a lens can be described as a double-diffraction process.

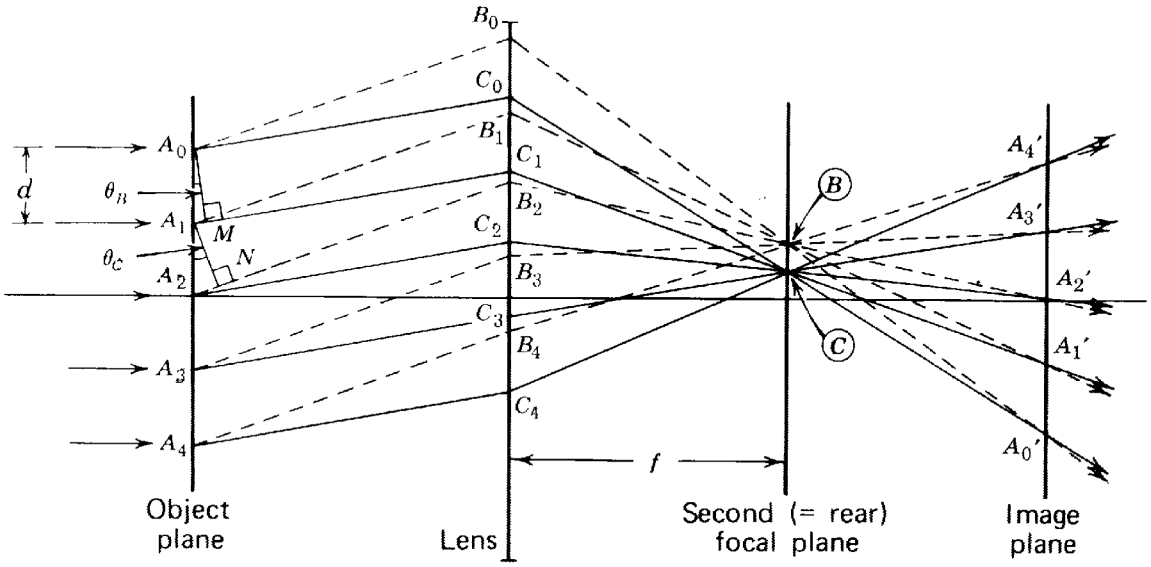

Fig. III.34. Imaging of a specimen with a periodic structure. (From Slayter, 1970, p.223)

Image formation is **analogous to Fourier analysis in the first stage, and Fourier synthesis in the second stage.** Fourier image analysis forms a powerful basis for analyzing a wide variety of periodic specimens because it separates the processing of electron micrograph images into two stages. The formation of the diffraction pattern in the first stage reveals structural information in a straightforward manner and conveniently and objectively separates most of the signal and noise components in the image. The transform may then be manipulated (§ III.D.2) and subsequently back-transformed in the second stage to produce a noise-filtered, reconstructed image.

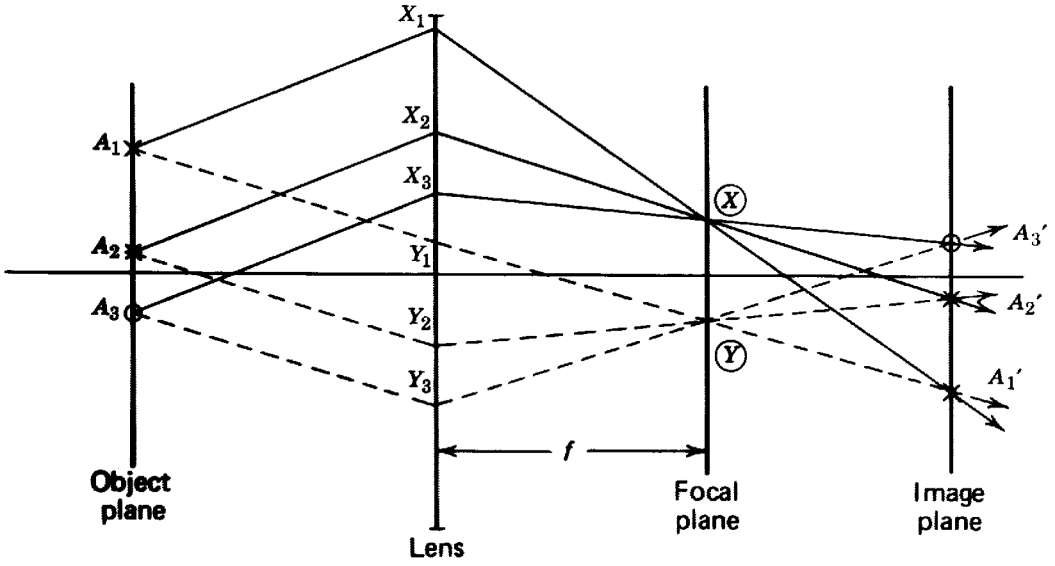

Fig. III.35. Imaging of a specimen with an irregular structure. (From Slayter, 1970, p.224)

e. Bragg diffraction

W. L. Bragg's simple description of the diffraction from crystals helps clarify our understanding of diffraction (Figs. III.36 and III.37). **Diffraction** can be visualized as arising from the **reflection** of radiation from planes of electron density in the 3D crystal (or lines in a 2D crystal). These lattice planes are imaginary parallel planes within crystals. Each set of planes is identified by three **Miller indices**, *hkl*. These indices are the reciprocals of the intercepts in units of cell edge lengths that the plane makes with the axes of the unit cell (Fig. III.38). Diffraction from the *hkl* set of planes, which are separated a distance d_{hkl}, only occurs for certain orientations of the incident radiation according to the Bragg relation: (see also p. 119, § I.F.1.a).

$$n\lambda = 2d_{hkl}\sin\theta_{hkl} \qquad \text{(III.C.6.6)}$$

where n = integer
λ = wavelength of incident radiation
d_{hkl} = crystal lattice spacing between the [*hkl*] set of crystal planes
θ_{hkl} = angle of incidence and also of reflection

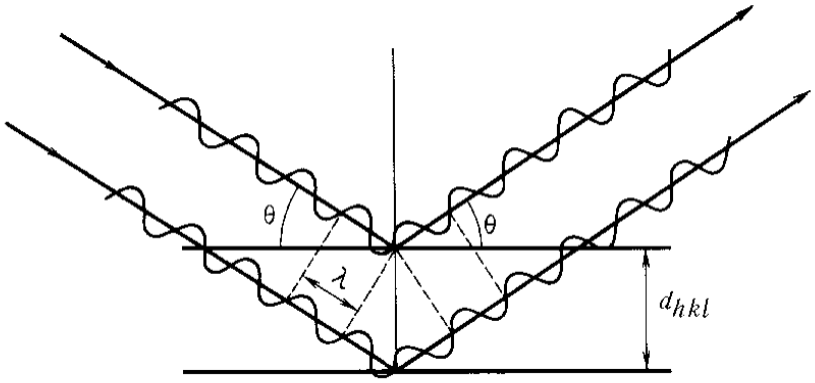

Fig. III.36. Bragg's law. θ is the angle of incidence and reflection; λ is the wavelength of the incident radiation; d_{hkl} is the spacing between the set of planes that is diffracting the incident radiation. (From Vainshtein, 1981, p.224)

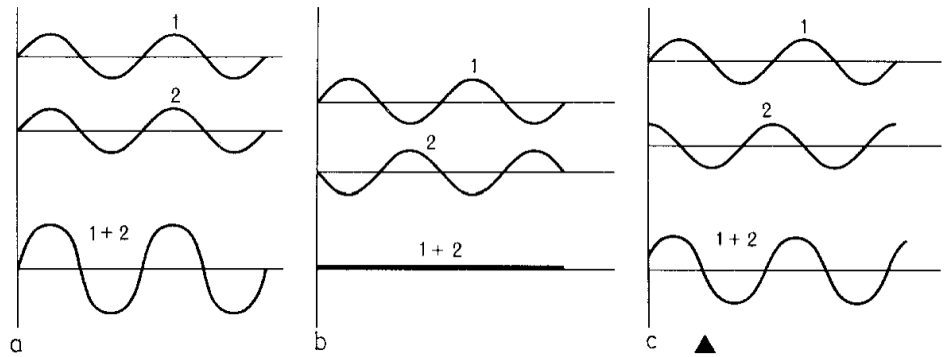

Fig. III.37. Interaction of two waves (1) and (2) with the same amplitude. (a) Doubling of the amplitude when the waves are in phase, (b) mutual annihilation of the waves in counter-phase, (c) change of amplitude and phase in general case of a phase shift. (From Vainshtein, 1981, p.224)

The **intensity** of each *hkl* reflection is <u>proportional to the distribution of electron density in the *hkl* planes</u>**.** In other words, in some planes the density may be evenly distributed and the

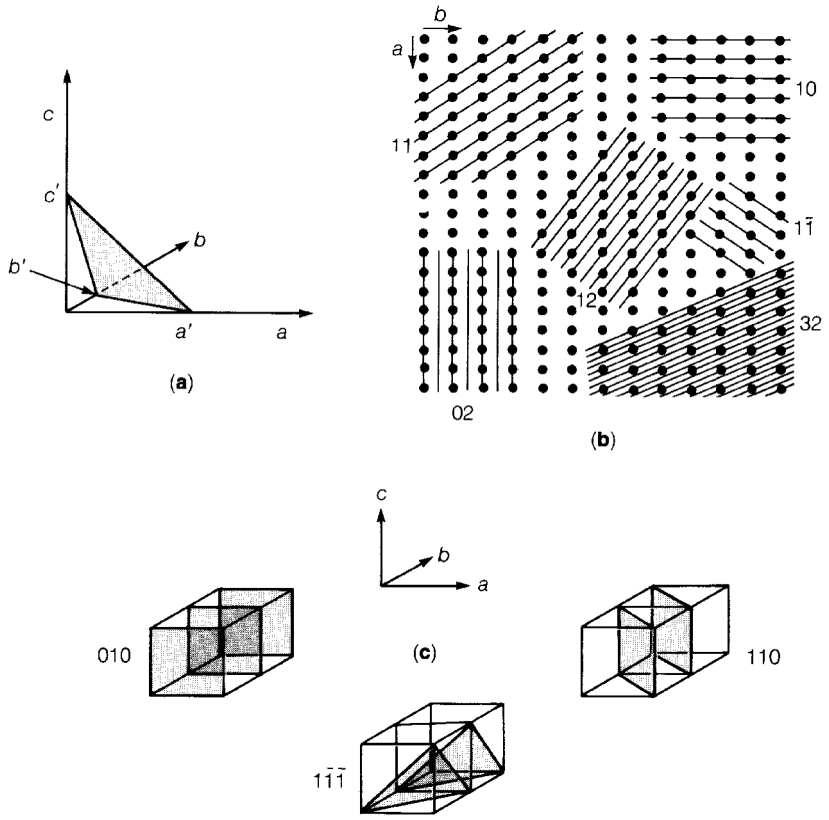

Fig. III.38. Miller indices of lattice planes in a crystal. (a) A lattice plane with intercepts a', b', and c' along the a, b, and c axes. (b) Lattice planes in a 2D lattice. (c) Lattice planes in a 3D lattice. (From Eisenberg and Crothers, 1979, p.811)

corresponding reflection will be relatively weak. If in others, the density is concentrated in one region between the planes, the corresponding reflection will be strong.

Two Bragg-type planes are depicted in the 2D crystal of hands (Fig. III.39, left). Densities that lie between the dashed lines diffract at the reciprocal lattice point labeled [1,2] (and also its **Friedel mate,** [-1,-2], not shown). The spacing or perpendicular distance between the lines is **inversely proportional** to the distance of the [1,2] reciprocal lattice point from the origin of the transform. Also, relative to the transform origin (where $\theta_{hkl} = 0°$, which corresponds to the direction of **unscattered** radiation), the reciprocal lattice point appears in a direction normal to the set of lines. The dotted lines in Fig. III.39 (left) represent the [2,3] set of lattice planes.

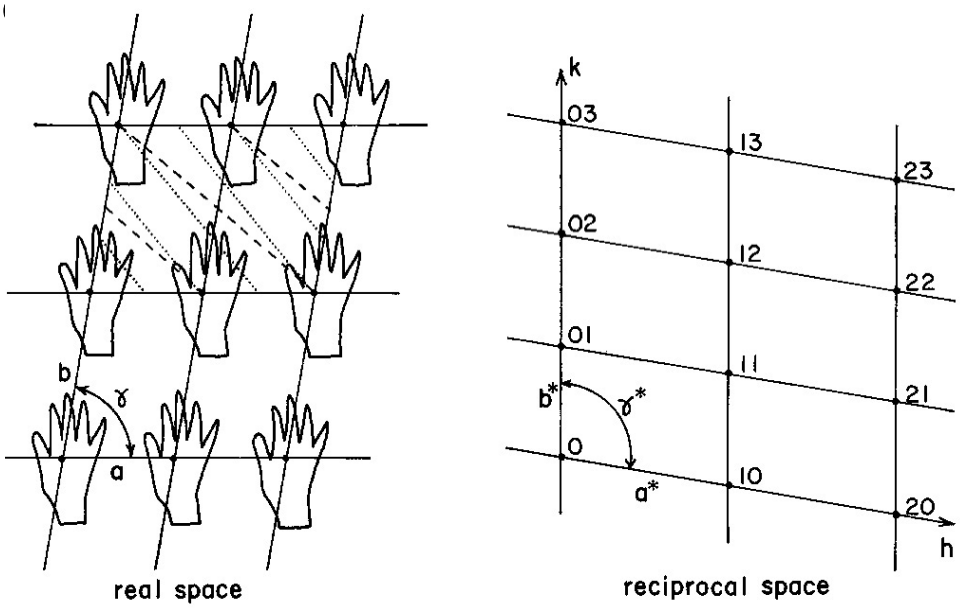

Fig.III.39. (Left) Two-dimensional crystal (P1 plane group) of hands. The unit cell dimensions, a and b, and the cell angle, γ, are shown as are a few sets of Miller 'planes'. (Right) Corresponding depiction of a quadrant of the reciprocal lattice that corresponds to the hand crystal at the left.

For 2D, periodic structures, each **Friedel pair** of spots arises from a set of fringes (sinusoidal density waves) of particular spacing (frequency) and orientation in the crystal. The so-called **Miller index** of each spot corresponds to the two wave numbers (*h* and *k*) that describe the number of wave cycles per repeat in the *a* and *b* directions. For example, the [2,3] set of waves (dotted lines in Fig. III.39) cross the *a* axis twice and the *b* axis three times in each unit cell.

In diffraction from 3D crystals, the Miller index of each spot is assigned three wave numbers (*h,k,l*) corresponding to the number of wave cycles per repeat in the three unit cell directions (*a,b,c*) (Fig. III.38c).

Each spot or reflection in the diffraction pattern may be **mathematically represented as a plane wave** whose amplitude is proportional to the square root of the spot intensity and whose phase is measured relative to a particular origin point in the crystal (*e.g.* the unit cell origin). The phase for a particular spot is the distance from the crest of the density wave to a chosen origin (Fig. III.30). When the amplitudes and phases (structure factors, F_{hkl}) of all spots in the 3D transform are known, the corresponding density waves can be mathematically summed (Fourier synthesis) to reconstruct the 3D object density (Figs. III.31 and III.32).

f. Structure factor

For a crystal, the structure factor describes the scattering of all atoms of the unit cell for a given Bragg reflection. Each diffracted ray, or reflection, is described by a structure factor, F_{hkl}. It is a **complex number** whose **magnitude** is proportional to the square root of the **intensity** of the *hkl* reflection. Each structure factor may be regarded as a sum of the contributions of the radiation scattered in the same direction from all atoms within the unit cell. The mathematical formulation of the structure factor depends on whether the object is considered to be continuous or made of a discrete number of atoms.

Objects consisting of discrete atoms

For **an object with *n* atoms,** the structure factor equation is:

$$F_{hkl} = \sum_{j=1}^{n} f_j \exp\left[2\pi i\left(hx_j + ky_j + lz_j\right)\right] \qquad \text{(III.C.6.7)}$$

where f_j is the **atomic scattering factor for atom j.** This is the ratio of the amplitude scattered by the atom to the amplitude scattered by a single electron in the atom. At zero scattering angle, f_j = atomic number, but, as the scattering angle increases, the value of f_j decreases because of the finite volume over which the electrons in the atom extend. The particular set of diffracting planes is designated by *hkl*, and x_j,y_j,z_j are the fractional unit cell coordinates for

each of the atoms in the unit cell.

Since $e^{i\theta} = \cos\theta + i\sin\theta$, equation III.C.6.7 can be rewritten:

$$F_{hkl} = \sum_{j=1}^{n} f_j \left\{ \cos\left[2\pi\left(hx_j + ky_j + lz_j\right)\right] + i\sin\left[2\pi\left(hx_j + ky_j + lz_j\right)\right] \right\} \quad \text{(III.C.6.8)}$$

$$= \sum_{j=1}^{n} f_j \cos\left[2\pi\left(hx_j + ky_j + lz_j\right)\right] + i\sum_{j=1}^{n} f_j \sin\left[2\pi\left(hx_j + ky_j + lz_j\right)\right] \quad \text{(III.C.6.9)}$$

$$= A_{hkl} + iB_{hkl} \quad \text{(III.C.6.10)}$$

We see therefore, that the structure factor F_{hkl} is a complex quantity, with **real** and **imaginary** components represented by A_{hkl} and B_{hkl}, respectively.

Argand diagram

F_{hkl} is conveniently depicted as a vector in an **Argand diagram** in which the horizontal axis represents the **real axis** and the vertical axis represents the **imaginary axis** (Fig. III.40). In this representation, the vector quantity F_{hkl} can be thought of as composed of the vector sum of A_{hkl}, the **real component,** and B_{hkl}, the **imaginary component.** The vector F_{hkl} makes an angle α_{hkl} with respect to the real axis. The magnitudes of the vectors A_{hkl} and B_{hkl} are, respectively, $|F_{hkl}|\cos(\alpha_{hkl})$ and $|F_{hkl}|\sin(\alpha_{hkl})$.

The **structure factor amplitude** is defined as the modulus or magnitude of F_{hkl}. That is:

$$|F_{hkl}| = [(A_{hkl})^2 + (B_{hkl})^2]^{1/2} \quad \text{(III.C.6.11)}$$

The **structure factor phase** of F_{hkl} is equal to the angle α_{hkl}.

$$\text{Since} \quad F_{hkl} = A_{hkl} + iB_{hkl} \quad \text{(III.C.6.12)}$$

$$= |F_{hkl}|\cos(\alpha_{hkl}) + |F_{hkl}|i\sin(\alpha_{hkl}) \quad \text{(III.C.6.13)}$$

$$= |F_{hkl}|\exp(i\alpha_{hkl}) \quad \text{(III.C.6.14)}$$

If θ_j is substituted for $2\pi(hx_j+ky_j+lz_j)$, the structure factor equation can be expressed in a simpler form:

$$F_{hkl} = \sum_{j=1}^{n} f_j e^{i\theta_j} \quad \text{(III.C.6.15)}$$

$$= \sum_{j=1}^{n} f_j\left(\cos\theta_j + i\sin\theta_j\right) \quad \text{(III.C.6.16)}$$

Structure with continuous density

For a 3D structure with **continuous density,** $\rho(xyz)$, the structure factor equation becomes:

$$F_{hkl} = V\int\int\int \rho(xyz)\exp^{2\pi i(hx+ky+lz)}\,dx\,dy\,dz \quad \text{(III.C.6.17)}$$

In this expression, the integration is over the entire unit cell volume, V. This reemphasizes a property we already know from the definition of the Fourier transform, namely, that **every point in the object contributes to every point in the diffraction pattern.**

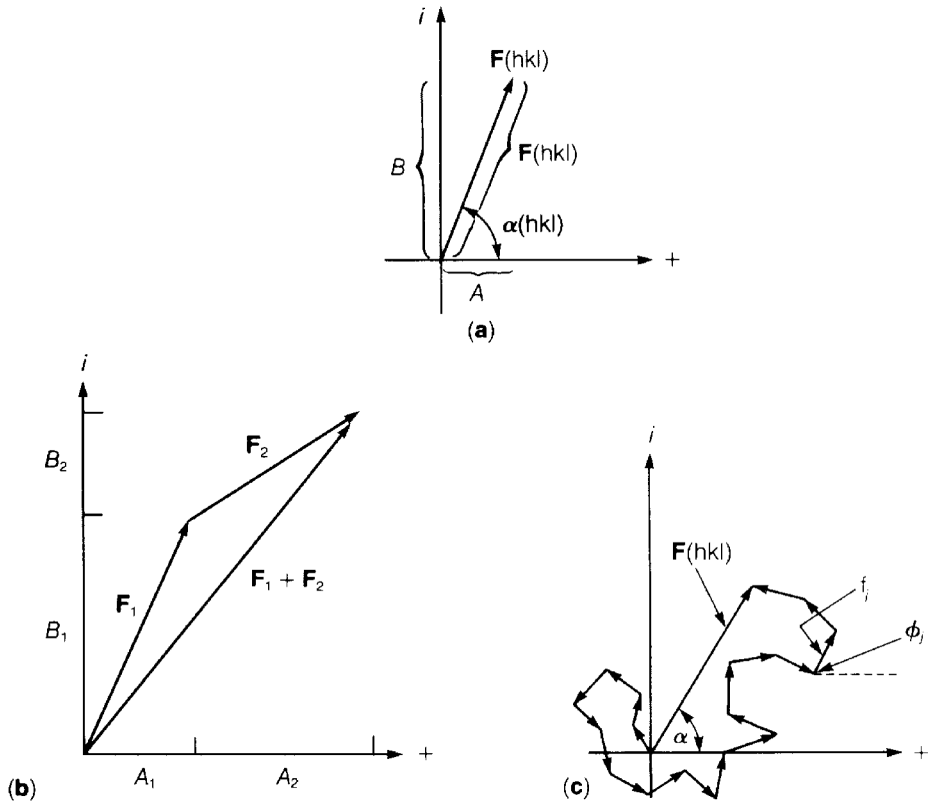

Fig. III.40. Argand diagram. Representation of structure factors by vectors in the complex plane. (**a**) The structure factor magnitude **F**(hkl) is represented by the length of a vector in the complex plane. The phase angle α(hkl) is given by the angle, measured counterclockwise, between the positive real axis and the vector **F**. (**b**) Complex numbers can be added by adding their real and complex components. (**c**) The structure factor for a reflection may be thought of as the vector sum of the scattering contributions from many atoms. Each of the *j* contributions may be represented as a vector in the complex plane, with amplitude f_j and phase ϕ_j. (From Eisenberg and Crothers, 1979, p.822)

g. Convolution and multiplication (sampling)

These concepts provide a fundamental basis for understanding diffraction from crystalline objects. Holmes and Blow (1965) give a general statement of the operation of convolution of two functions:

> *"Set down the origin of the first function in every possible position of the second, multiply the value of the first function in each position by the value of the second at that point and take the sum of all such possible operations."*

This is expressed in mathematical terms as:

$$c(u) = \int_{-\infty}^{\infty} f(x)g(u-x)dx \qquad \text{(III.C.6.18)}$$

This is known as the **convolution** of $f(x)$ and $g(x)$, and may be written as:

$$c(u) = f(x) * g(x) \qquad \text{(III.C.6.19)}$$

Several examples of convolution are schematically depicted in Figs. III.41-43.

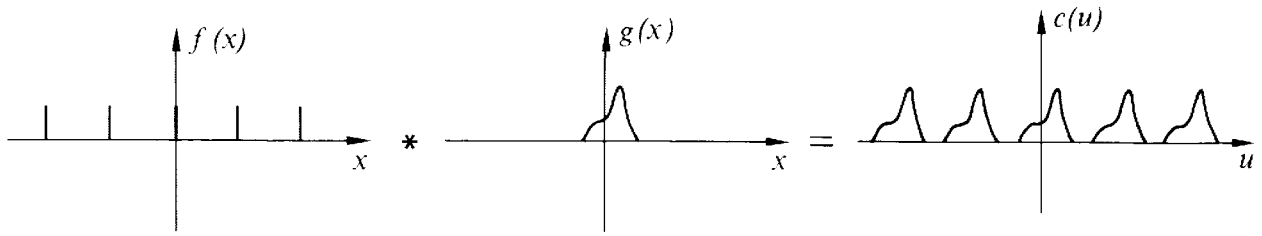

Fig. III.41. Convolution with an array of δ functions. If *f(x)* is an array of δ functions, and *g(x)* an arbitrary function like that shown, then the result of the convolution *f(x)* * *g(x)* is to associate the *g* function with each δ function. This is always true on condition that *g(x)* is narrower than the spacing of the δ functions so that *g(x)* never overlaps two δ functions simultaneously. (From Sherwood, 1976, p.173)

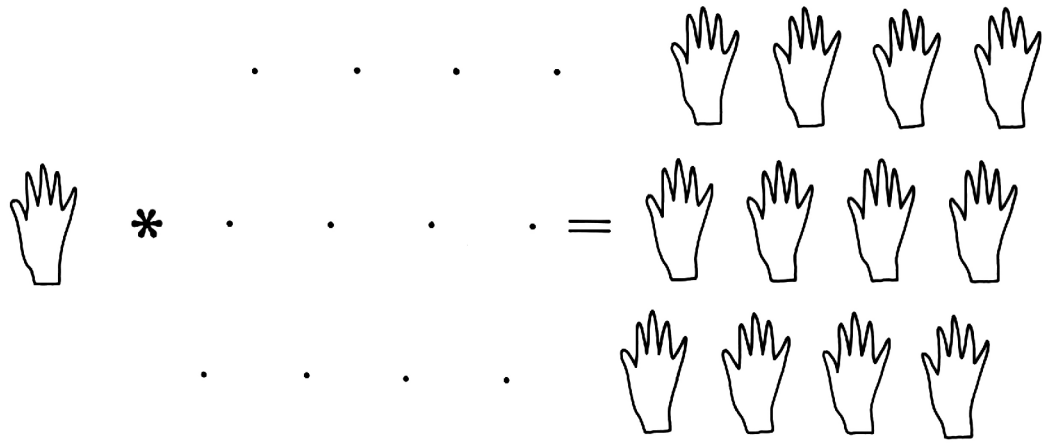

Fig. III.42. The convolution of a right hand (palm down) with a finite, 2D lattice gives rise to a finite, 2D crystal structure.

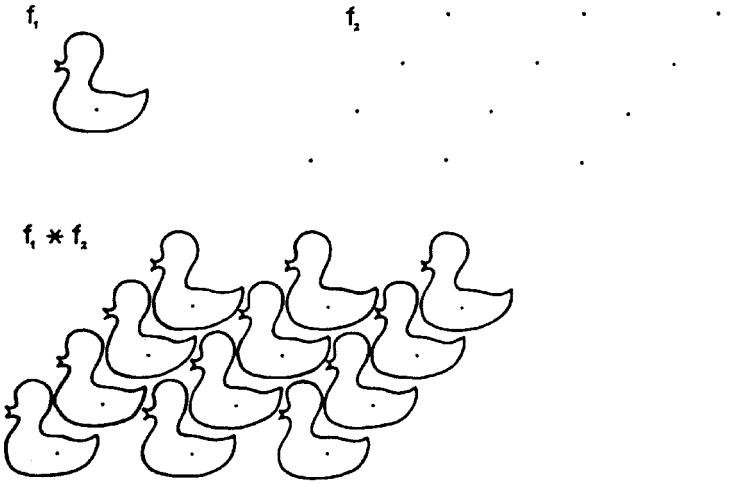

Fig. III.43. A simple example of convolution. One function, $\mathbf{f_1}$, is a drawing of a duck, the other, $\mathbf{f_2}$, is a 2D lattice. The convolution of these functions is accomplished by putting the duck on every lattice point. (From Holmes and Blow, 1965, p.123)

The **convolution theorem** provides a precise way to describe the relationship between objects in real space and transforms in reciprocal space. It states that the Fourier transform of the convolution of two functions is the product of their Fourier transforms.

$$T(f * g) = F \times G \qquad \text{(III.C.6.20)}$$

The converse of the above also holds, namely that the Fourier transform of the product of two functions is equal to the convolution of the transforms of the individual functions.

$$T(f \times g) = F * G \qquad \text{(III.C.6.21)}$$

The symbols, $*$ and x, correspond to the convolution and multiplication operations. The two functions are represented by *f* and *g*, and ***F*** and ***G*** are their respective Fourier transforms.

The convolution of a motif (f_1) with a finite lattice (f_2) to produce a crystal structure (f_3) is

illustrated in Fig. III.42 and Fig. III.43. These examples are easy to conceptualize because, in each case, one of the functions (here it is f_2) is a lattice. Fortunately, most periodic specimens we are considering obey this restriction. A **crystal structure** is thus equivalent to the convolution of a finite lattice with the contents of the unit cell**.** Mathematical computation of the convolution of two functions is usually required when **neither** function is a lattice.

All of the objects depicted in Fig. III.44(a,c,e,g) can be described as convolutions of a motif and a 1D lattice. In these examples, a hand motif is convoluted with one, two, three or ten-point (*i.e.* finite), horizontal lattices. The diffraction patterns to the right of each "object" (Fig. III.44b,d,f,h) demonstrate the properties of transforms as formulated in the convolution theorem, namely:

$$T(f_3) = T(f_1 * f_2) = F_3 = F_1 \times F_2 \quad \text{(III.C.6.22)}$$

$$T^{-1}(F_3) = T^{-1}(F_1 \times F_2) = f_3 = f_1 * f_2 \quad \text{(III.C.6.23)}$$

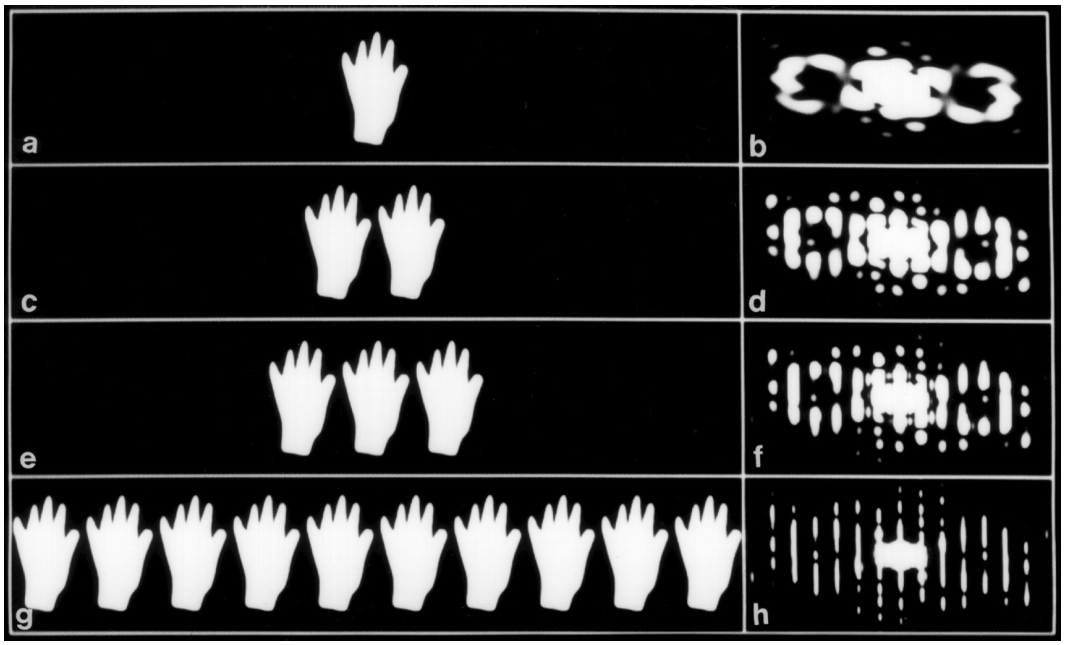

Fig. III.44. Lattice sampling. (a) A single left hand (palm facing down) and (b) its diffraction pattern. (c) Two hands and (d) their diffraction pattern. Note that this is a sampled version of the transform shown in **b**. (e) Three hands and (f) their diffraction pattern, which is a more sharply sampled version of transform **b**. (g) Row of ten hands and (h) its diffraction pattern. This transform is the most sharply sampled version of transform **b**.

In other words, the transform of the crystal structure, F_3, is the transform of the unit cell contents (a single hand), F_1, multiplied (sampled) by the transform of the crystal lattice, F_2 (reciprocal lattice: the sampling interval is reciprocally related to the real space lattice repeat, *i.e.* the distance separating the hands). The transform of the contents of the unit cell is a **continuous function** (Fig. III.44b), whereas the transform from the crystal is **discrete** (Fig. III.44d,f,h). That is, the crystal transform is the transform of the single unit cell "sampled" at the reciprocal lattice positions. Values of the Fourier transform at the reciprocal lattice positions are called the **structure factors,** F_{hkl} (§ III.C.6.f).

The transform of Fig. III.44c, shown in Fig. III.44d, is the transform of a single hand (Fig. III.44b) multiplied by the transform of a two-point lattice (series of thick, vertical lines). Note in Figs. III.44d,f,h that the thickness of the vertical "sampling" lines in each of these transforms is inversely proportional to the number of hands or points in the finite lattice (Note that an *infinite* lattice would produce *infinitely thin* lines). In Figs. III.44d,f,h the transform of a single hand (Fig. III.44b) is **sampled** by the vertical fringes of the reciprocal lattice function. The hand transform (Fig. III.44b) is similarly described as the transform of a single hand sampled by an **infinitely thick,** vertical fringe (transform of a single point).

Also notice in Fig. III.44 that the 1D lattices give rise to transforms sampled in only one direction, whereas 2D lattices produce sampling on a 2D grid or **reciprocal lattice.** Thus, transforms of 2D crystals are the individual object transforms sampled at the reciprocal lattice points (Fig. III.45). If the phase and amplitude (structure factor) at each point *hk* in the reciprocal lattice can be obtained, the crystal and motif structures can be solved by mathematical Fourier synthesis (equivalent to an inverse Fourier transformation). Figs. III.46 and III.47 show additional examples of convolution and sampling as given in the text by Sherwood (1976).

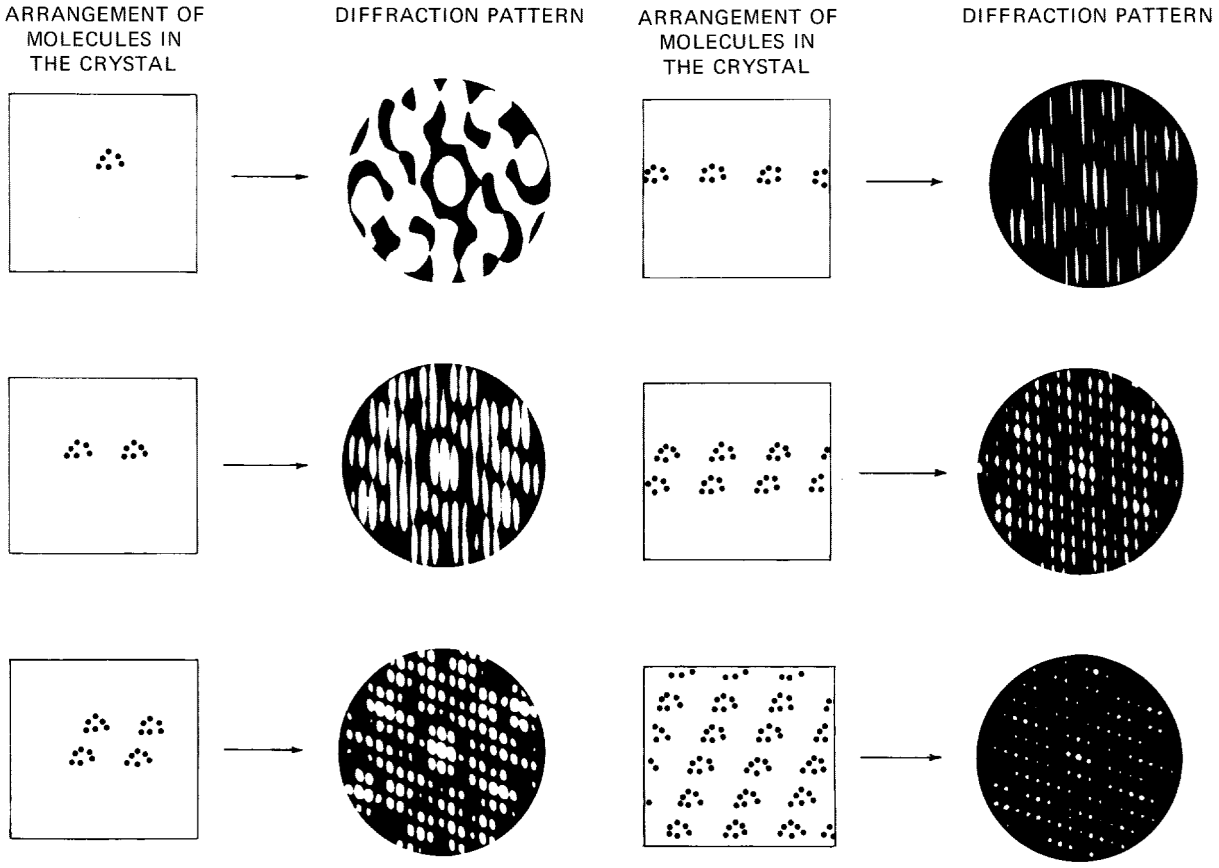

Fig. III.45. Relationship between the diffraction pattern of a "molecule" and various regular arrangements of such molecules. (a) A single molecule. (b) Two molecules horizontally side by side. (c) Four molecules arranged in a parallelogram. (d) Many molecules horizontally side by side (a 1D crystal). (e) Two rows of molecules arranged on an oblique lattice. Only parts of the rows are shown. (f) 2D crystal of molecules. Only part of crystal is shown. (From Glusker and Trueblood, 1972, pp.28-29)

h. Other properties of Fourier transforms and diffraction patterns

Optical diffraction / "mathematical" transform analogy

An optical bench is an excellent device for demonstrating the properties of diffraction patterns and Fourier transforms and provides a clear analogy between X-ray and Fraunhofer diffraction. Taylor and Lipson (1964) and Harburn, Taylor and Welberry (1975) present hundreds of examples of objects and their optical diffraction patterns. These examples provide a solid foundation for understanding, at least within a visual framework, the principles of diffraction theory. In optical diffraction experiments (discussed later in § III.D.1), the diffraction grating or object may be a photographic transparency or an opaque material in which holes have been punched or etched out, and the incident radiation is a visible laser beam. The relationship between object structure (real space) and its transform (reciprocal space) will be illustrated in several figures in the following pages.

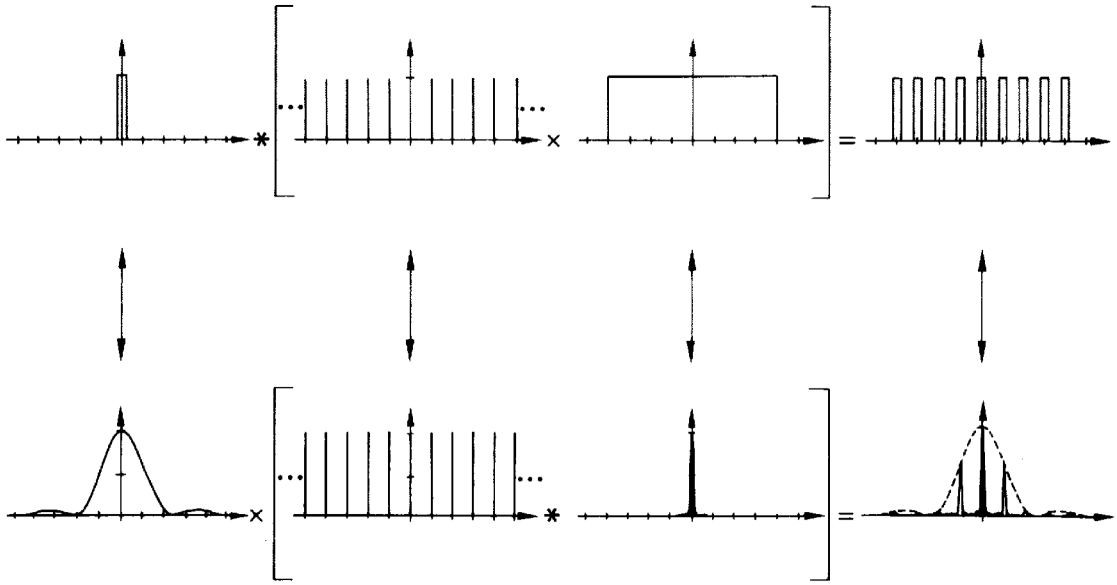

Fig. III.46. Diffraction pattern of N wide slits, showing Fourier transform and convolution relationships. Objects are shown in the top row and corresponding diffraction patterns on the bottom row. The diffraction patterns are shown in more detail in Fig. III.47. (From Sherwood, 1976, p.255)

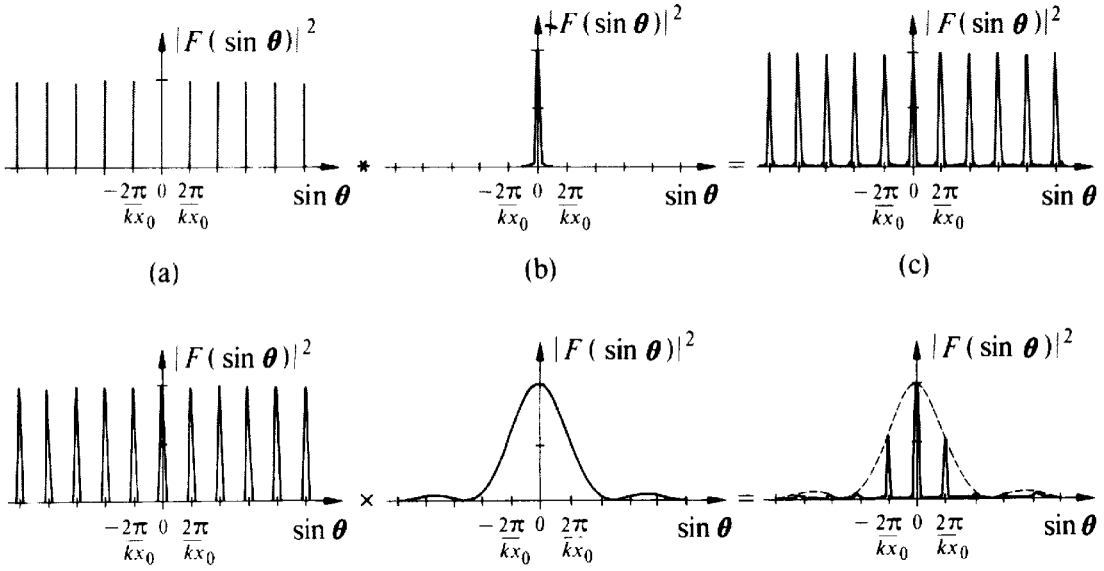

Fig. III.47. Diffraction pattern of N wide slits. The diffraction patterns of an infinite array of delta functions and of the boundary function are shown in (a) and (b), respectively, and their convolution gives rise to (c), the diffraction pattern of N narrow slits. On multiplying this by the pattern of one wide slit shown in (e), we derive (f), the diffraction pattern of N wide slits. (From Sherwood, 1976, p.254)

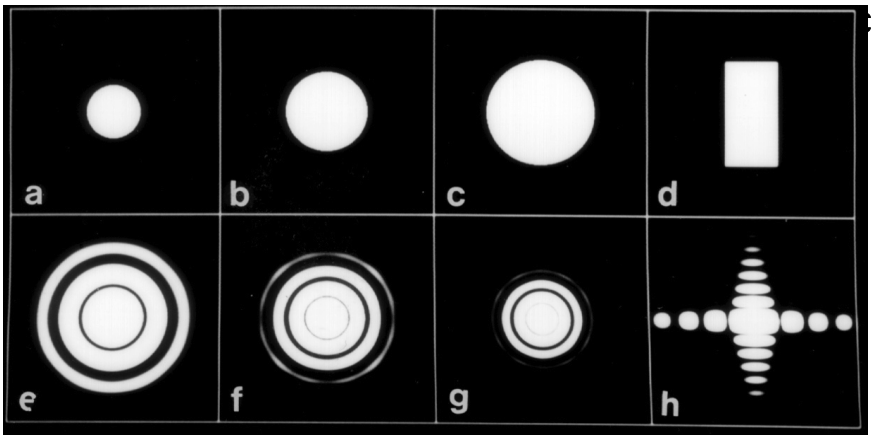

Fig. III.48. (a) Small, (b) medium, and (c) large circular disks and their respective Fourier transforms (e-g). (d) Rectangle and (h) its Fourier transform.

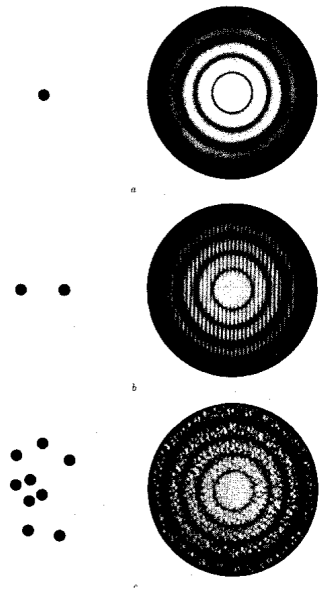

Fig. III.49. (a) A disk and its diffraction pattern. (b) Two disks and their diffraction pattern. (c) A random array of disks and their diffraction pattern. (From Holmes and Blow, 1965, p.119)

Asymmetric vs. symmetric structures and their transforms

Simple, symmetric structures (Fig. III.48a-d and Fig. III.49 upper left) generally produce simple, symmetric transforms (Fig. III.48e-h and Fig. III.49 upper right), whereas asymmetric structures generally produce transforms that are more complex (Figs. III.49-51). Transforms are like **fingerprints** in the sense that specific object features often give rise to characteristic features in the transform. Each structure can be regenerated by back transformation **only** if the amplitudes and phases at **all points** of the transform are available. This may be accomplished for visible light (optical reconstruction, § III.D.2) or for electrons (electron microscopy), but can only be achieved by mathematical computation for X-rays and neutrons where phases are indirectly measured.

Some shapes (Fig. III.48a-d) may be directly deduced from characteristic transforms (Fig. III.48e-h). Simple inspection of most transforms (Figs. III.49 bottom row and Figs. III.50 and 51) though, does not directly lead to a unique determination of structure.

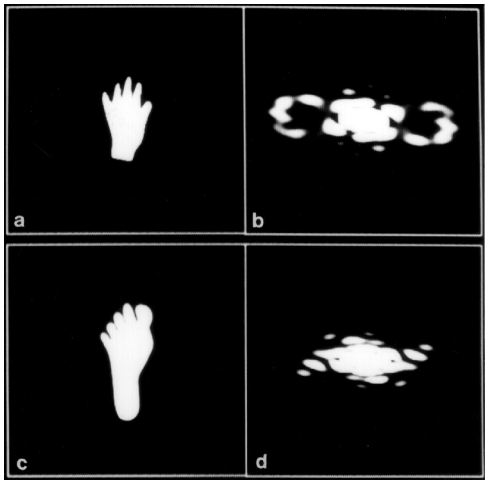

Fig. III.50. (a) Hand and (b) its Fourier transform. (c) Foot and (d) its Fourier transform.

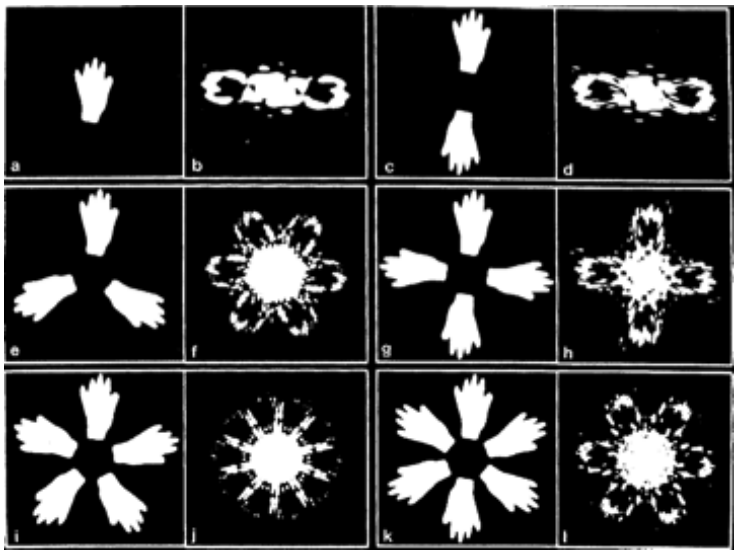

Fig. III.51. A series of objects with rotational symmetries C_1, C_2, C_3, C_4, C_5, C_6, (a,c,e,g,i,k) and their respective transforms (b,d,f,h,j,l).

Reciprocity

Dimensions in the **object (REAL SPACE)** are **inversely related to dimensions in** the **transform (RECIPROCAL SPACE).** Thus, features that are spaced far apart in reciprocal space represent small spacings or features in real space. For a circle, as its diameter increases the diffraction rings become smaller and narrower (Fig. III.48a,b,c,e,f,g). The close, vertical edges of the rectangular object (Fig. III.48d) produce widely spaced fringes in the horizontal spike of the transform (Fig. III.48h), and the wide, horizontal edges of the box produce closely spaced fringes in the vertical spike. Reciprocity is also illustrated by examples shown in Figs. III.39, 50 and 51.

Resolution

Outer regions of the transform arise from fine **(high resolution)** details in the object. Conversely, **coarse object features** contribute near the central **(low resolution)** region of the transform. Unscattered rays (those scattered through an angle of zero degrees) appear at the exact center of the transform. For example, by blocking out portions of the hand transform (Fig. III.52a) and allowing the remaining rays to recombine to form an image (equivalent to optical filtering, § III.D.2), we can demonstrate that the fingers are fine details (Fig. III.52b,c,e), whereas the hand as a whole is a coarse feature (Fig. III.52f,g). As high-resolution information is removed from the transform, fine structural details (fingers) are no longer distinguished in the reconstructions. This procedure is called low-pass filtering to denote that the low-resolution features (near the center of the transform) are allowed to interfere (resynthesize) at the image plane whereas the high-resolution features are removed (see also Fig. III.53). Removal of, or blocking out the low resolution Fourier components leads to edge enhancement, which is just an accentuation of the high-resolution features (edges) (Fig. III.52d).

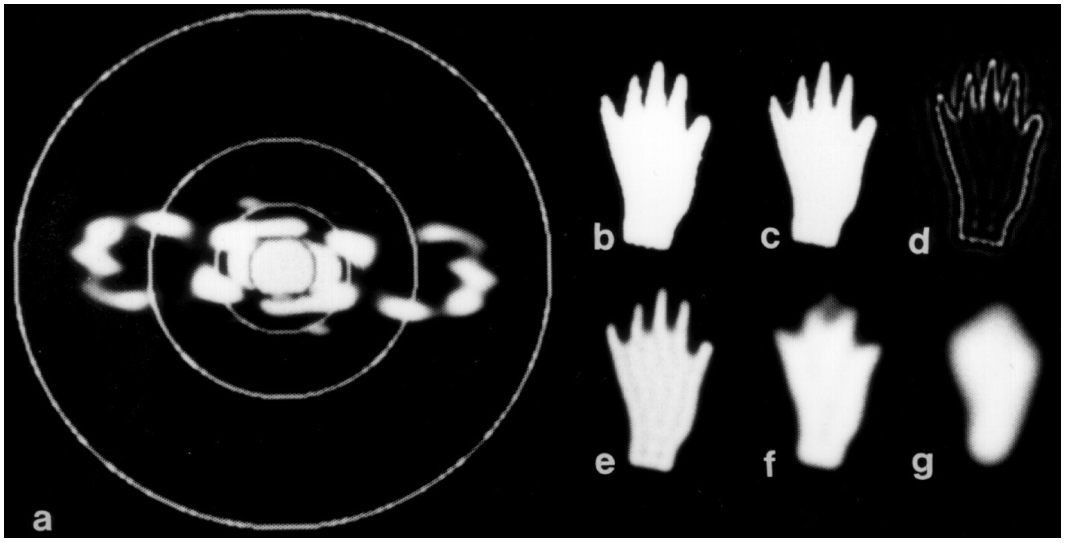

Fig. III.52. (a) Fourier transform of a single hand. Rings denote the extent to which regions of the transform are allowed to recombine to form either low-pass (b,c,e,f,g) or high-pass (d) filtered image reconstructions.

Sharpness of diffraction spots

Features in the diffraction pattern **get sharper** as the **number** of diffracting objects or the **distance** between them increases (Figs. III.44, 54 and 55). As the horizontal, 1D 'crystals' increase in size by adding more units (Figs. III.44 and III.55) or by increased separation between units (Fig. III.54), the vertical fringes sharpen in the diffraction pattern. Sharpening reflects a situation of more complete, destructive interference away from the reciprocal lattice positions. The inverse relationship between sharpness and overall object size (extent) is another example of the reciprocity between object (real) and diffraction (reciprocal) space.

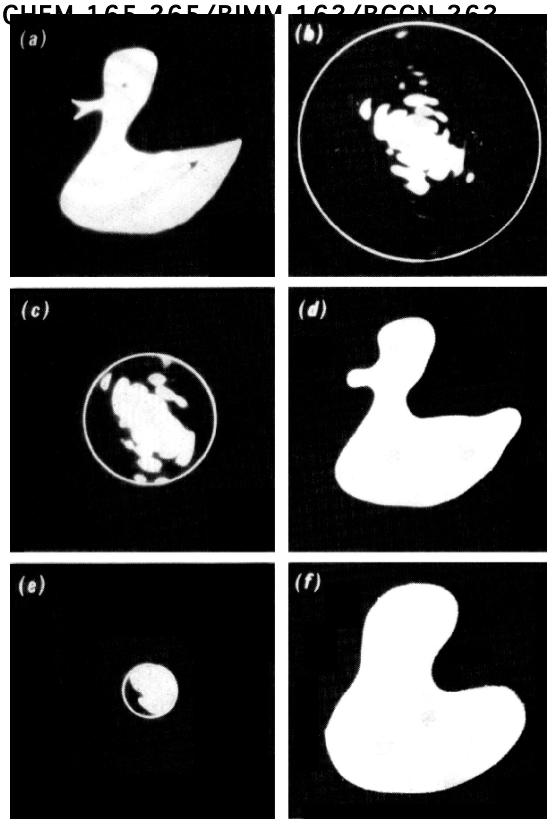

Fig. III.53. Similar to Fig. III.52, showing the effect of taking only low angle diffraction to form the image of a duck object. A drawing of a duck is shown, together with its diffraction pattern. Also shown are the images formed (as the diffraction pattern of the diffraction pattern) when stops are used to cut progressively more of the high angle diffraction pattern. (From Holmes and Blow, 1965, p.120)

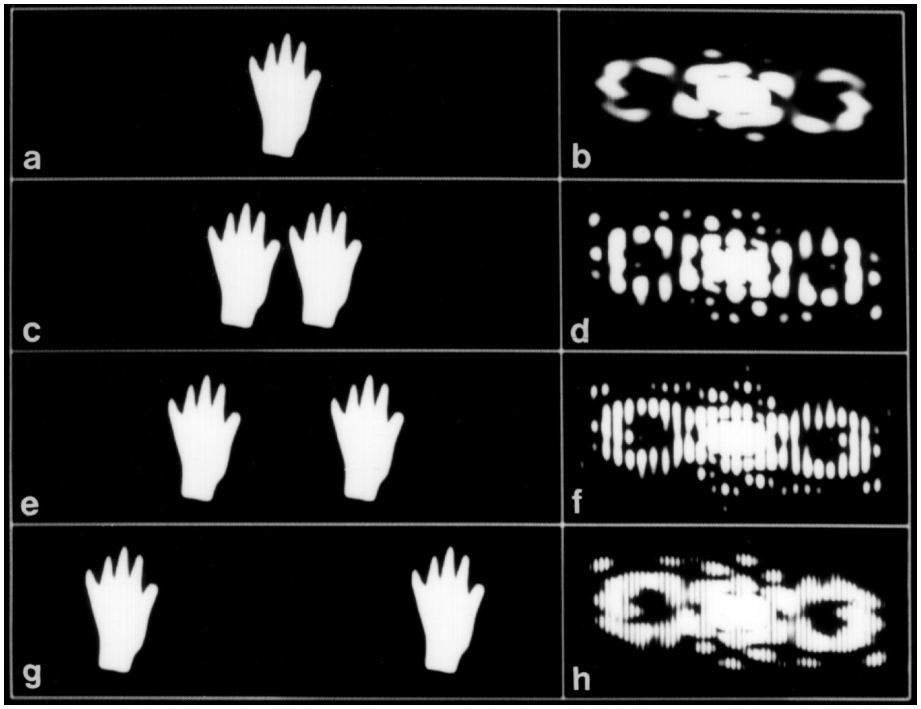

Fig. III.54. Effect of object separation on transform. (a) Single hand and its transform (b). (c,e,f) Pair of hands at increasing separation and the respective Fourier transforms (d,f,h).

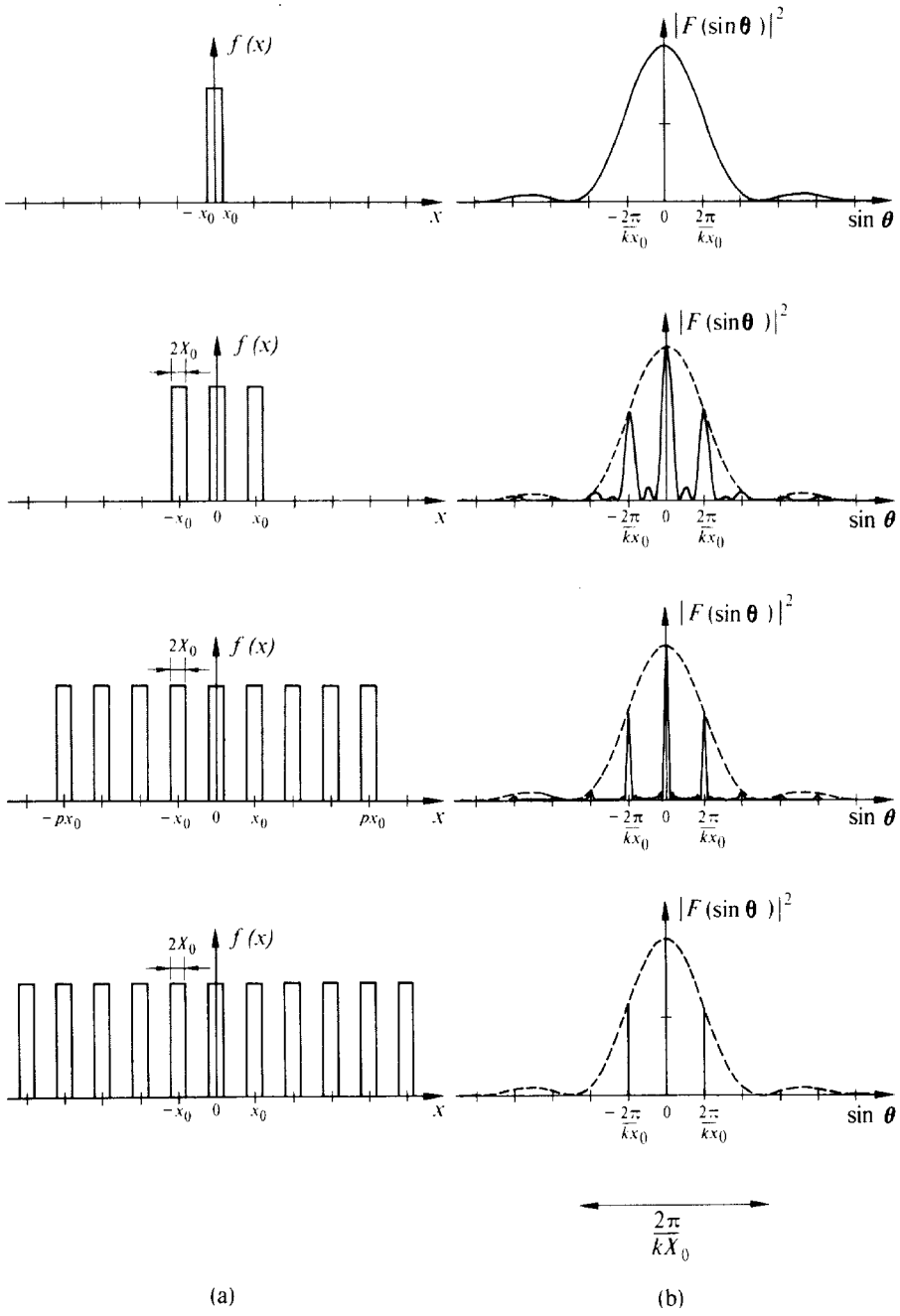

Fig. III.55. Significance of the diffraction pattern. The amplitude functions for one, three, N, and ∞ wide slits are depicted in (a), and the respective diffraction patterns in (b). Introducing a motif has the effect of altering the intensities of the main peaks, but the positions of these peaks remain the same, for the lattice determines this. Also, the shape of each main peak remains the same for this is a function of the overall shape of the entire molecule. (From Sherwood, 1976, p.249)

Geometry, intensity and symmetry

The relative orientation and dimensions between real and reciprocal space lattices for a 2D crystal are illustrated in Figs. III.39, 45, 56, and 57. Parameters of the crystal lattice and reciprocal lattice are related by:

$$d^* = K/(d \sin\gamma^*) \qquad \text{(III.C.6.24)}$$

and $$\gamma^* = 180\text{-}\gamma \qquad \text{(III.C.6.25)}$$

K is the constant of diffraction (= λL, where λ is the wavelength of monochromatic radiation and L is the camera length, *i.e.* the distance from the specimen to the diffraction plane).

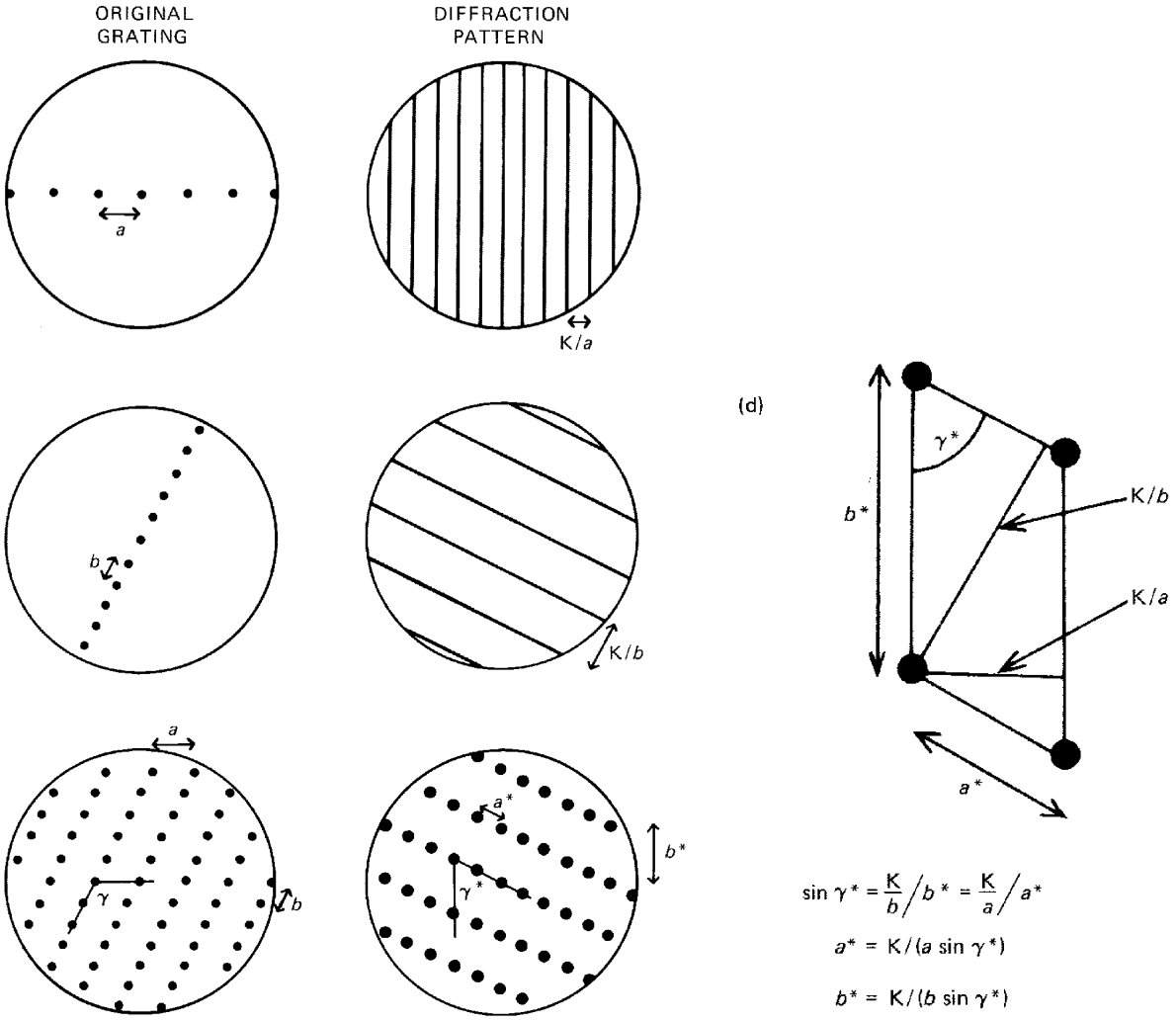

Fig. III.56. (a-c) Diagrams of gratings are shown on the left and the corresponding diffraction patterns (such as might be obtained by holding each grating in front of a point source of light) are shown on the right. **a and b** are direct lattice vectors in the crystal or grating and ***a**** and ***b**** are vectors in the diffraction pattern. The reciprocal relationships of ***a*** and ***b*** to the spacings of certain rows in the diffraction pattern are shown. The fact that the intensity is the same at all reciprocal lattice points in the diffraction pattern in (c) should NOT be thought to be general; it happens here because the scattering objects in the original "crystal lattice" are all particularly simple (isotropic holes) and are much smaller than the wave-length of the radiation used in this hypothetical experiment. Consequently, the intensities of the diffraction maxima show no variation in different directions and do not vary significantly with angle of scattering (which increases with increasing distance from the center of the pattern). (d) The relationships of ***a*** and ***b*** to ***a**** and ***b**** are shown. The lattice spacings, ***a**** and ***b****, in this 2D reciprocal lattice are of great importance in diffraction experiments. For a particular diffraction pattern, the scale factor K depends upon the wavelength of the radiation used and upon the geometry of the experimental arrangement. (From Glusker and Trueblood, 1972, pp.24-25)

Notice that the **reciprocal lattice directions**, with dimensions a^* and b^*, are respectively perpendicular to the cell edges ***b*** and ***a***. In Fig. III.39 it is important to note that **ONLY** the positions and **NOT** the relative intensities of the Bragg reflections are depicted. However, relative intensities are depicted in Fig. III.45. Each spot is indexed according to its position in the reciprocal lattice, and is considered to arise by diffraction from a set of density planes (or lines for 2D) in the crystal.

Comparisons of Figs. III.44 and III.54, and Fig. III.50 demonstrate that the **structure of the motif** and **NOT the spacings or geometry of the crystal lattice** determine the intensity distribution in the transform**.**

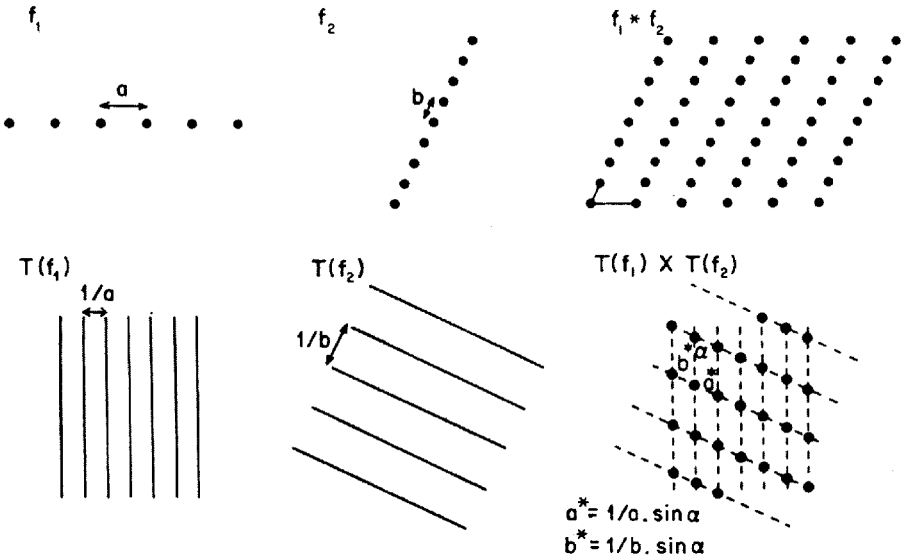

Fig. III.57. The buildup of a lattice by convoluting two rows of points, and of the reciprocal lattice by multiplying together the transform of the two rows of points, which is two sets of lines. (From Holmes and Blow, 1965, p.127)

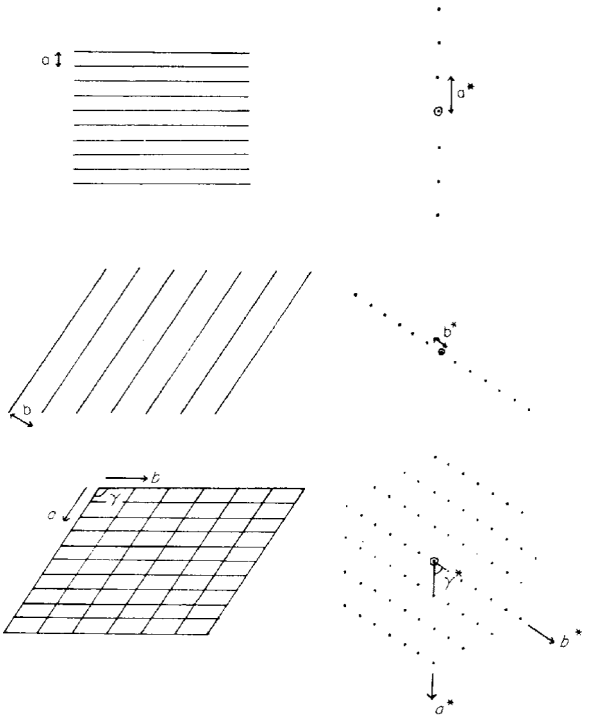

Fig. III.58. The transform of a set of lines and of a lattice. (From Blundell and Johnson, 1976, p.114)

Structural symmetry produces symmetrical intensity distributions in the transform (aside from Friedel symmetry, see below). Fig. III.51, for example, clearly illustrates that symmetric objects produce symmetric transforms. This property is one of the major reasons why optical diffraction (§ III.D.1) is a powerful method for diagnosing in TEM images the presence of symmetry in biological specimens.

Objects with rotational symmetry (Fig. III.51a,c,e,g,i,k) give rise to transforms with the same *n*-fold symmetry if the *n* is an even-order number, or 2*n*-fold symmetry if *n* is an odd number. In these examples, the transform of the asymmetric unit (one hand, Fig. III.50a) is not sampled in the symmetric transforms because the motifs (Fig. III.51c,e,g,i,k) are not crystals. That is, the asymmetric units are not in identical orientations strictly related by translations.

Screw-axis symmetry in a crystal produces systematic absences in the transforms. The transforms of crystals with vertical or horizontal dyad screw-axes (2_1) appear with every other spot missing in the vertical or horizontal rows (shown with slides in class).

Not shown are examples of crystalline objects with symmetric motifs. One might envision a crystal with the motif of Fig. III.51g placed at the points of a square lattice. The transform of such a crystal is the transform of the motif (Fig. III.51h) sampled at the points of a square reciprocal lattice ($a^*=b^*$, $\gamma^*=90°$). In this example, the asymmetric unit of the crystal is just one hand (one-quarter of the motif) because the four-fold motif symmetry matches the four-fold lattice symmetry.

Projection theorem

The projection theorem states that the Fourier transform of the projected structure of a 3D object is equivalent to a 2D central section of the 3D Fourier transform of the object**.** The central section intersects the origin of the 3D transform and is perpendicular to the direction of projection. Optical transforms of projected specimen images are, therefore, 2D slices through the complete 3D transform of the specimen. This forms the basis of 3D reconstruction by Fourier methods, where several independent views of the projected structure are recorded and their transforms calculated to build up a complete 3D transform (Fig. III.59). The 3D structure is reconstructed from the 2D views by inverse Fourier transformation of the complete transform.

Friedel's law

Friedel's law states that there is an **inversion center** in the intensity distribution in the diffraction pattern from the projected structure of a **real** object**.** This means that the amplitude at any point in the pattern is identical at a point equidistant and opposite in direction from the transform origin. The **phases** at these two points are **opposite.** For periodic specimens with periodic patterns consisting of discrete spots (reflections), Friedel related spots are called Friedel pairs.

In X-ray diffraction, Friedel's law breaks down under conditions where there are atoms that scatter anomalously (refer to any basic text on X-ray diffraction methods for a detailed explanation). In optical diffraction experiments, Friedel's law generally breaks down (*i.e.* the pattern does not show perfect inversion symmetry in the intensity distribution) because the object is a photographic transparency, which causes phase shifts of the incident radiation (laser light) as it passes through the emulsion and backing of the film. It is possible (although quite messy!) to reduce these phase effects by using specially designed optical systems in which the transparency and diffraction lens are combined in a way in which the transparency can be immersed in an oil of refractive index closely matching the refractive index of both the transparency and lens.

Mathematically computed diffraction patterns should always show **perfect** Friedel symmetry (*e.g.* Figs. III.44, 45, 48, 50-54, and 59), that is of course, assuming the primary computed calculations are bug-free!

III.C.7. References Cited in §III.C.

Bernal, I., W. C. Hamilton, and J. S. Ricci (1972) Symmetry: A Stereoscopic Guide for Chemists, p. 180, W. H. Freeman and Co., San Francisco.

Blundell, T. L., and L. N. Johnson (1976) Protein Crystallography, p. 565, Academic Press, N. Y.

Buerger, M. J. (1971) Introduction to Crystal Geometry, (McGraw-Hill series in materials science and engineering) p. 204, McGraw-Hill, New York.

Eisenberg, D. and D. Crothers (1979) In Physical Chemistry with Applications to the Life Sciences, Benjamin/Cummings Pub. Co., Inc., Menlo Park, Calif. **pp. 749-797**.

Glusker, J. P., and K. N. Trueblood (1972) Crystal Structure Analysis: A Primer, p. 192, Oxford University Press, New York.

Henry, N. F. M., and K. Lonsdale, Eds. (1969) International Tables for X-ray Crystallography. (Vol 1: Symmetry Groups), p. 558. The Kynoch Press, Brimingham, England.

Holmes, K. C. and D. M. Blow (1965) The use of X-ray diffraction in the study of protein and nucleic acid structure. *Meth. Biochem. Anal.* **13:113-239.**

Lake, J. A. (1972) Biological studies, pp. 153-188, *In* H. Lipson, Ed., Optical Transforms. Academic Press, London.

Sherwood, D. (1976) Crystals, X-rays and Proteins, p. 702, John Wiley & Sons, New York.

Slayter, E. M. (1970) Optical Methods in Biology, p. 757, John Wiley & Sons, New York.

Vainshtein, B. K. (1981) Modern Crystallography I: Symmetry of Crystals, Methods of Structural Crystallography, (Vol 15: Springer Series in Solid-State Sciences) M. Cardona, P. Fulde and H.-J. Queisser, Eds., p. 399, Springer-Verlag, Berlin.

Wilson, H. R. (1966) Diffraction of X-rays by Proteins, Nucleic Acids and Viruses, p. 137, Edward Arnold Pub. Ltd., London.

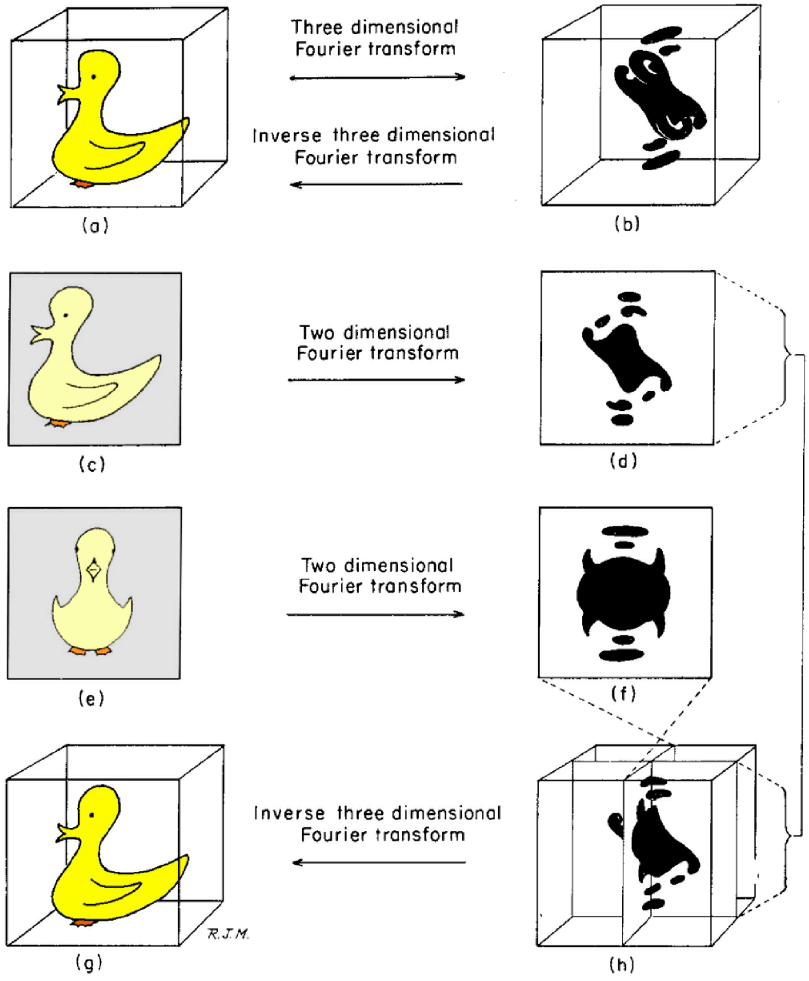

Fig. III.59. The mathematical principles of 3D reconstruction. (a) A 3D duck and (b) its 3D Fourier transform; (c) A projection of (a) and (d) the 2D Fourier transform of (c); (e) Another projection of (a) and (f) its 2D Fourier transform; (g) The 3D duck calculated from the 3D Fourier transform (h) which was reconstructed by sampling 3D Fourier space with the 2D transforms (d) and (f). (Modified from Lake, 1972, p.174)